# 國立交通大學

## 資訊學院 資訊學程

## 碩 士 論 文

快速 OFDM 訊框時間差估計方法之設計與其在
無線中繼網路降低換手頻率之研究

Fast OFDM Frame Inter-Arrival Time Differences Estimation
and Its Application to Handoff Reduction in Wireless Relay Networks

研 究 生：陳政敏

指導教授：王蒞君 教授

曾煜棋 教授

中 華 民 國 九 十 七 年 七 月

快速 OFDM 訊框時間差估計方法之設計與其在
無線中繼網路降低換手頻率之研究
# Fast OFDM Frame Inter-Arrival Time Differences Estimation
# and Its Application to Handoff Reduction in Wireless Relay Networks
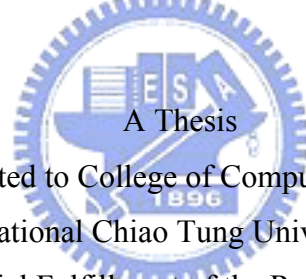
研 究 生：陳政敏　　　　　Student：Cheng-Min Chen

指導教授：王蒞君　　　　　Advisor：Dr. Li-Chun Wang

　　　　曾煜棋　　　　　　　　　　Dr. Yu-Chee Tseng

國 立 交 通 大 學
資訊學院　資訊學程
碩 士 論 文

A Thesis

Submitted to College of Computer Science

National Chiao Tung University

in partial Fulfillment of the Requirements

for the Degree of

Master of Science
in
Computer Science

July 2008

Hsinchu, Taiwan, Republic of China

中華民國九十七年七月

快速 OFDM 訊框時間差估計方法之設計與其在
無線中繼網路降低換手頻率之研究

學生：陳政敏　　　　　　　　　　　　　　指導教授：王蒞君 教授
　　　　　　　　　　　　　　　　　　　　　　　　　曾煜棋 教授

國 立 交 通 大 學　　資 訊 學 院　　資 訊 學 程 碩 士 班

摘　　　要

　　　　本論文係研究在一個廣泛佈建 OFDM 無線中繼網路的都會區域中，快速移動的用戶端設備遭遇換手次數頻繁之問題，並提出相關的解決方案。在 OFDM 無線中繼網路中，引入一個新的網路元件—中繼站(Relay Station)，用以改善因建築物遮蔽所產生的訊號品質衰落問題，並藉以提高訊號涵蓋範圍。中繼站具備完整訊框結構，對基站(Base Station)而言，中繼站被視為一個用戶端(Mobile Station)；對用戶端而言，中繼站扮演基站的角色。隨著中繼站佈建數量的增加，快速移動的用戶端將面臨換手次數提高的問題。

　　　　在一個以 OFDM 為基礎的通信系統中，訊框同步是個重要的議題。對於一個快速移動的用戶端而言，此問題尤其嚴重。但接收機在處理訊框同步過程中所估算到的訊框長度差，卻恰好可作為反應基站(含中繼站)與用戶端之間相對運動的參數。基於此參數，我們設計一個新的換手目標選擇指標，以有效的抑制換手次數的提升。

　　　　本論文的第一部分提出一個基於實體層的快速訊框到達時間估算方法。OFDM 無線中繼網路的訊框結構中，不論是基站或中繼站，均擁有獨立的廣播標頭(Preamble)。此標頭以 BPSK 調變，在通過 IFFT 區塊之後，會呈現獨特的對稱特性。藉此特性，我們可以完成訊框到達事件偵測，並得到 FFT 長度與循環字首(Cyclic Prefix)的長度，而不須預先經過 MAC 層控制信令傳送給接收機端。藉由上述實體層資訊，我們可以估測訊框到達時間以及訊框長度，並與系統預設之訊框長度作比較後可以得到訊框時間差。

　　　　本論文第二部份設計一個新的換手目標選擇指標，並實作一個模擬都會區域廣泛佈建中繼站的類曼哈頓(Manhattan-like)模擬器。此模擬器實做 IEEE 802.16j 相關實體層參數、信號衰落模型，以驗證新指標的性能。模擬結果顯示此新指標能有效抑制換手頻率，對於降低換手次數有顯著的效果。

# Fast OFDM Frame Inter-Arrival Time Differences Estimation and Its Application to Handoff Reduction in Wireless Relay Networks

Student：Cheng-Min Chen          Advisors：Dr. Li-Chun Wang
                                            Dr. Yu-Chee Tseng

Degree Program of Computer Science
National Chiao Tung University

## ABSTRACT

In this thesis, we investigate how to efficiently using the relative movement information of MS to reduce handoff event and control signaling overhead for OFDM-Based wireless relay networks. In wireless relay networks, the relay station (RS) is introduced to improve the link quality and coverage. However, RS may cause the increase handoffs when an MS moves across the boundary between RS and BS, thereby result in signaling overhead for handoff. A handoff algorithm in wireless relay networks should intelligently reduce unnecessary handoffs.

Firstly, we develop a frame arrival event detection and frame arrival time estimation algorithm based on fast PHY-layer Schemes for obtaining cyclic prefix (CP) Lengths and fast Fourier transform (FFT) Sizes. Traditionally, CP length and FFT size are broadcasted via media access control (MAC) layer to pre-handoff MS. The algorithm we proposed is based on the conjugated symmetry characteristics of binary phase shift keying (BPSK) modulated preamble.

Secondly, the difference of the estimated consequent frame inter-arrival time could be used to judge that MS moves toward a RS or leaving away a RS. This is called the relative movement information, which is considered to develop a time-of-arrival based target selection algorithm for handoff procedure.

In simulated Manhattan-like urban model, physical layer parameters, path-loss model and handoff procedure of IEEE 802.16j are implemented. We evaluate the performance of the proposed algorithm. Our result shows that proposed algorithm can reduce the handoff frequency significantly compared to traditional signal-based target selection.

# 誌　　　謝

我的論文，終於告個段落。要不是上帝的眷顧，我無法度過無數個台北新竹來回奔波的夜晚。從小就覺得讀書不是件容易的事，為了很多原因，我堅持了下來。但其中最重要的，是家人(父、母、兄、妹)的支持與鼓勵，沒有他們作為心靈上的後盾，我沒有辦法撐過來。

我要感謝我的指導教授－王蒞君教授。我與老師研討論文的過程，堪稱夙夜匪懈。老師精確的檢視論文的內容，並指出裡頭的邏輯錯誤。沒有老師的指導，我無法完成這些。我也要感謝我的共同指導教授－曾煜棋教授。因為曾教授願意擔任共同指導，我才有機會從資工領域跨入通信領域。

此外，實驗室裡的建華學長、維正學長、中瑋學長、偉賢，給了許多研究上的協助及建議，感謝上帝讓我遇見這麼多好人與這麼多金頭腦。

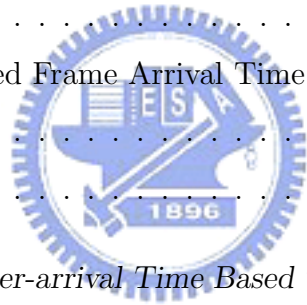身為一個來自花蓮的阿美族人，我也要將此份論文獻給吉安鄉娜荳蘭部落的族人親友與祖靈。但願這份論文，也帶著一些山與海的味道。

<div align="right">－Adop</div>

# Contents

# List of Tables

# List of Figures

# CHAPTER 1

# Introduction

The orthogonal frequency division multiplexing (OFDM) based systems have become a main stream in the next generation communication system, such as 3rd generation partnership project long term evolution (3GPP LTE), 3rd generation partnership project 2 air interface evolution (3GPP2 AIE) and worldwide interoperability for microwave access (WiMAX). For above systems, there are two identical features in them: higher transmission rate and more intelligent functions. Their common characteristic is that OFDM-based technique is adopted in the physical layer.

OFDM possess many advantages. It converts a frequency selective fading channel into parallel collection of frequency flat fading sub-channels, thereby overcomes the inter-symbol interference (ISI). It also allows overlapped sub-carriers and maintains their orthogonality to achieve higher spectrum efficiency.

The OFDM-based IEEE 802.16 standard is designed for local and metropolitan area networks. The IEEE 802.16-2004 standard defines the air interface and medium control message for the fixed broadband wireless access systems. The IEEE 802.16e standard extends the application from the fixed system to the mobile system. The IEEE 802.16j standard is based on the IEEE 802.16e standard which introduced relay

station (RS) to improve link quality and system coverage. The RS forwards the signal from one station to another one or to the managed mobile station (MS). A new frame structure is designed to contain the subframe of RS in the downlink subframe of a base station (BS). In each subframe the preamble is used for synchronization between RS and MS. From the viewpoint of the MS, an RS looks like a BS. However, for the BS, an RS also looks like an MS. Thus the RS plays two roles in the IEEE 802.16j networks.

## 1.1  Problems and Solutions

In the metropolitan environment, the signals are reflected and shadowed by the building. Thus the link quality and coverage degrade rapidly. Deploying RSs widely can solve this problem. Since the RS acts as a BS, handoffs will be triggered when the signal strength is lower than the specific threshold. The more relay stations deployed, the higher handoff frequency we may have. Thus, signaling overheads increase and may interrupt upper layer application service [1]. The objective of this thesis is to design an efficient target selection algorithm to reduce handoff frequency and control signaling overhead.

The Fig. 1.1 shows an example while an MS needs to handoff. The conventional handoff algorithm depends on the received signal strength indicator (RSSI) to decide whether the handoff is necessary and determine the selected target station. The MS in the figure may handoff to $RS_2$ first and then handoff to $RS_1$. In fact, if the received signal strength from $RS_1$ is good enough, MS shall handoff to $RS_1$ directly. Thus it is unnecessary to trigger the handoff process to $RS_2$.

To solve this problem, we suggest to include the mobility pattern of MS in the target selection algorithm. The mobility pattern can be represented by the relative movement Indicator (RMI) according to the difference between observed frame inter-
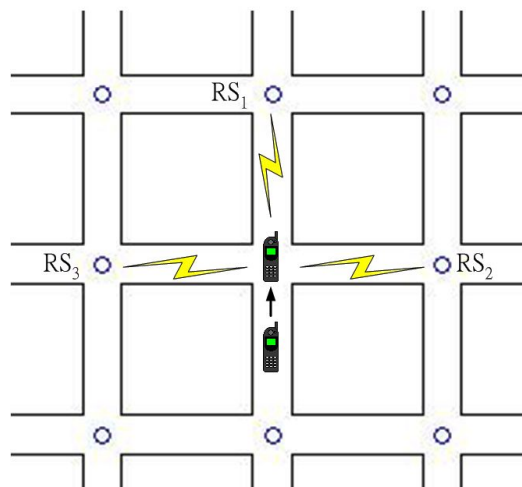
*Fig. 1.1:* A example of handoff scenario.

arrival time and the predefined frame inter-arrival time, which is called the difference of frame inter-arrival time. Since each sub-frame has the preamble for synchronization between RS and MS, RS looks like a BS for MS. Thus, regardless of a BS or RS the candidate target station is, the RMI can be estimated by the MS. By combining RSSI and RMI, the MS can select the best candidate target station with less unnecessary handoffs.

Next, we design a handoff evaluation indicator which integrates RSSI and RMI. When a handoff event is triggered, an MS must select a new target station. The new indicator helps an MS to choose the best target station which hold a longer connection time. With highly deployed RSs, the issue of target selection become very important. In Fig. 1.2, the difference of frame inter-arrival time between MS and $RS_1$ is larger than that between MS and $RS_2$. In this case, $RS_1$ has higher priority to become the target station for handoff.
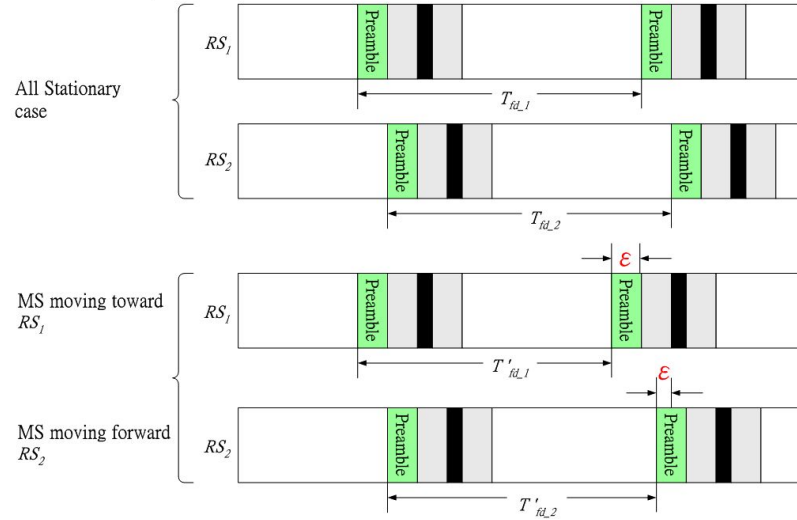
*Fig. 1.2:* Time difference of frame arrival caused by relative mobility.

## 1.1.1 OFDM Frame Arrival Time Estimation based on Fast PHY-layer Schemes for Obtaining CP Lengths and FFT Sizes

To estimate the difference of frame inter-arrival time, there are two important things should be discussed: frame arrival detection and frame arrival time estimation.

### Frame Arrival Detection and Estimation of FFT Sizes and CP Length

Frame arrival detection mechanism is to detect frame arrival event. The challenge lies in how to estimate fast Fourier transform (FFT) size and cyclic prefix (CP) length without the help from media access control (MAC) layer because the MS may not received the system control message from BS. We propose a frame arrival detection mechanism based on the fast PHY layer estimation of FFT size and CP length which are usually obtained from the MAC layer and cause long delay and signaling overhead.

**Frame Arrival Time Estimation**

The actual frame arrival time should be estimated after a receiver detects the frame arrival event and obtains the information of FFT size and CP length. Though OFDM is designed to overcome ISI, delayed signals from prior symbol still have the chance to interfere with next symbol when CP length is too short. We design a time domain pre-FFT equalizer to deal with this problem.

## 1.1.2 Difference of Frame Inter-arrival Time Based Target Selection Scheme for Reducing Handoffs in Wireless Multi-hop Relay Networks

In the Wireless multi-hop relay systems, the handoff decision and target selection decision are basically based on the RSSI. The handoff frequency will grow proportionally to the density of the deployed RS in the metropolitan environment. To solve this problem, we introduce the RMI into the target selection indicator. We integrate RSSI and RMI. For example, when an MS needs to handoff, and there exist two target stations with similar RSSI, an MS can choose the target station with larger RMI value even with smaller RSSI. The connection between MS and selected target station can be hold for a longer time. In our simulations, the proposed idea successfully decreases the handoff frequency.

## 1.2 Thesis Outline

In this thesis, we investigate how to reduce the handoff frequency, while MS moving in a metropolitan environment. We first design the frame arrival detection based on fast PHY layer scheme for obtaining FFT size and CP length. Next, We discuss how

to estimate the actual frame arrival time. By doing so, we can estimate the mobility pattern (i.e RMI) between the MS and candidate target stations. When considering both RMI and RSSI, we can help an MS to select a more suitable target station during handoff.

The remaining chapters of this thesis are organized as follows. In Chapter 2 we introduce the background of the physical layer in the IEEE 802.16 wireless metropolitan area network (WMAN). We introduce the frame structure and synchronization process for the handoff procedure. In Chapter 3, we provides a frame arrival detection algorithm for obtaining FFT size and CP length which based on the conjugated symmetric characteristics of The binary phase shift keying (BPSK) modulated preamble. Latter, we discusses the frame arrival time estimation algorithm in Chapter 4, and compare the performance of traditional algorithm and proposed algorithms under the AWGN channel and the SUI-3 channel. In Chapter 5, a novel RMI estimation algorithm is proposed. We simulate the proposed target selection algorithm for handoff in a Manhattan like urban environment, and give a comparison between traditional indicator and proposed indicator. At last, we give the concluding remarks and suggestions for future work in Chapter 6.

# CHAPTER 2

# Background

In this chapter, we introduce the background of the orthogonal frequency-division multiple access (OFDMA) physical layer in the IEEE 802.16 wireless metropolitan area network (WMAN). The concept of synchronization techniques, MAC message flow, and the channel model are also be introduced.
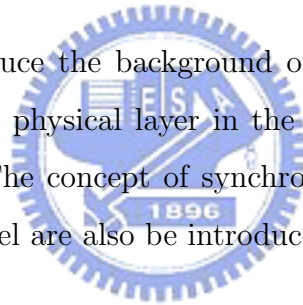
## 2.1 OFDMA Physical Layer in IEEE 802.16 Standard

The new radio technology-WiMAX is based on the wireless transmission methods defined by IEEE 802.16 standard. The IEEE 802.16 WirelessMAN [2] [3] specifies the standards for the air interface and MAC protocols for the fixed, portable, and mobile broadband wireless access systems. The typical application of the IEEE 802.16 WiMAX includes mesh networks, backhual, wireless digital subscriber line (DSL) to residential and small-office-and-home-office (SOHO), and broadband mobile networks.

The IEEE 802.16-2004 standard specifies OFDM as the transmission method.

The line of sight (LOS) link operates in the 10-66 GHz, and non-line-of-sight (NLOS) link operates in the 11 GHz. The OFDM signal is composed of many orthogonal carriers, and every carrier is modulated with a relatively slow symbol rate. This method has the advantages in a area with multipath channel because more time is needed to transmit a symbol compared to the single carrier method at the same transmission rate.

The guard period is added to the front of every symbol in OFDM-based signal, which is a short copy of the tail of original symbol. It can avoid the multipath effect to radio transmission. These characteristics result in a stable connection because of the very low bit error rate (BER). BPSK, quadrature phase shift keying (QPSK), 16 quadrature amplitude modulation (16QAM), and 64 quadrature amplitude modulation (64QAM) modulation modes are used, and the modulation scheme can be adapted to satisfy difference transmission conditions. The IEEE 802.16e standard is an expansion to satisfy the requirement of mobile application and roaming, and it frequency range is up to 6 GHz. The number of carriers can vary over a wide range depending on permutation zones and FFT size (128 to 2048 points).

The IEEE 802.16 standard specifies two flavors of OFDM systems: (1) OFDM and (2)OFDMA. The OFDM method aims at the short distance applications, such as indoors. The FFT size is 256. The downlink (DL) multiplex scheme is time-division multiplexed (TDM), and that in the uplink (UL) is time-division multiple access (TDMA). For OFDMA, the subcarrier in higher FFT size (2048 carriers) are divided into groups, which is called subchannels. It mapping the subcarriers into logical channels in downstream. Those sub-channels using different modulation, coding, and amplitude to fit different channel characteristics.

The IEEE 802.16-2004 and IEEE 802.16e standards have several channel bandwidths from 1.5 to 20 MHz. This can be adopted to the configuration of different tranciever platforms. Furthermore, this flexibility is also helpful for cell planning.
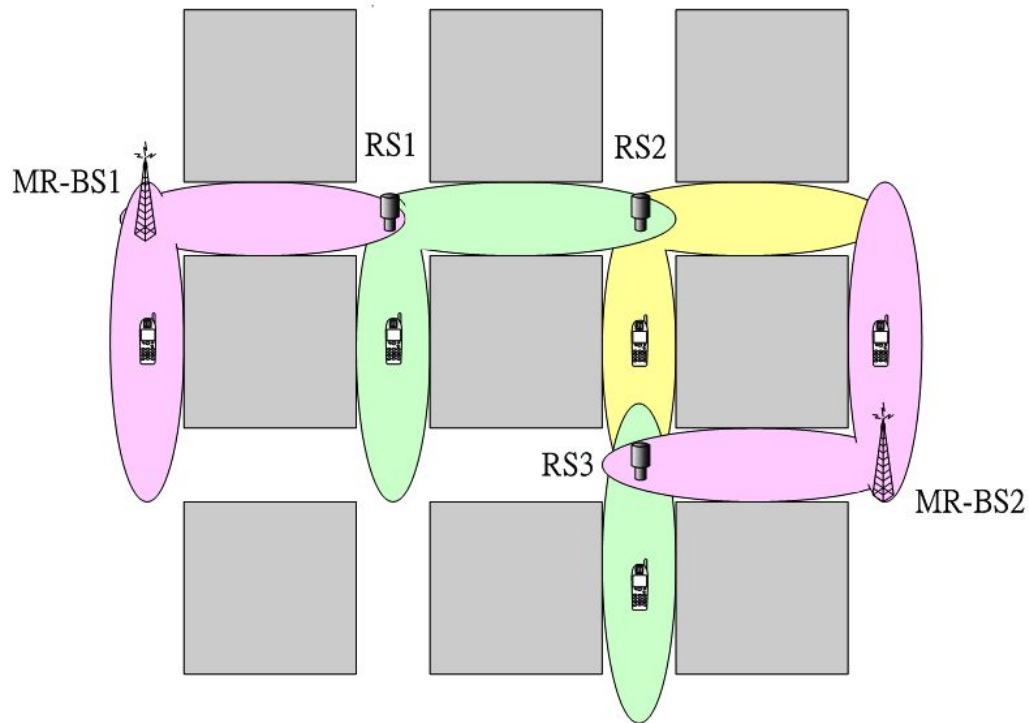
*Fig. 2.1:* A simple multi-hop relay network.

## 2.2 Introduction to IEEE 802.16j Multi-hop Relay Networks

The multi-hop relaying (MR) becomes an important technique for future wireless networks, which can extend the coverage or improve link quality specially in urban environment. A simple MR network is shown in Fig. 2.1.

In the wireless multi-hop relay networks, cell diameter is smaller than that in conventional cellular networks. The coverage of an RS is expected from 200 to 500 meters, thus the transmit power of an RS is smaller than that of multi-hop BS (MR-BS). The small size of coverage makes the deployment easier and more flexible

than that of MR-BS [4].

The IEEE 802.16j is a standard for specifying the wireless multi-hop relay operation used in metropolitan environment [5]. The RS can extend cell coverage, and allows for more efficient frequency reuse. In the reference [6], gives a summary of the usage models for IEEE 802.16j networks. The purpose of usage models is to define different deployment scenarios (such as fixed, nomadic, mobile) to fit the requirements of network elements (such as RS) and functional entities to improve system performance.

The usage models are classified from the perspective of the infrastructure. The usage model maps the different services into different infrastructures. It define four usage models as follow:

1. Fixed Infrastructure Usage Model (I)

    In this usage model, the main purpose of deploying RS is coverage expansion. Besides, improving the capacity or per user throughput in areas which are not sufficiently covered by the MR-BS. See the Fig. 2.2.

2. In-Building Coverage Usage Model (II)

    In this usage model, an RS provides a better coverage and higher throughput inside the building, tunnel or underground such as on a subway platform. See the Fig. 2.3.

3. Temporary Coverage Usage Model (III)

    In this usage model, an RS is deployed temporarily to cover a region which is not included in the original cell planning. See the Fig. 2.4.

4. Coverage on Mobile Vehicle Usage Model (IV)

    In this usage model, an RS is deployed in a mobile vehicle which provides MS a stable backhual connection. See the Fig. 2.5.
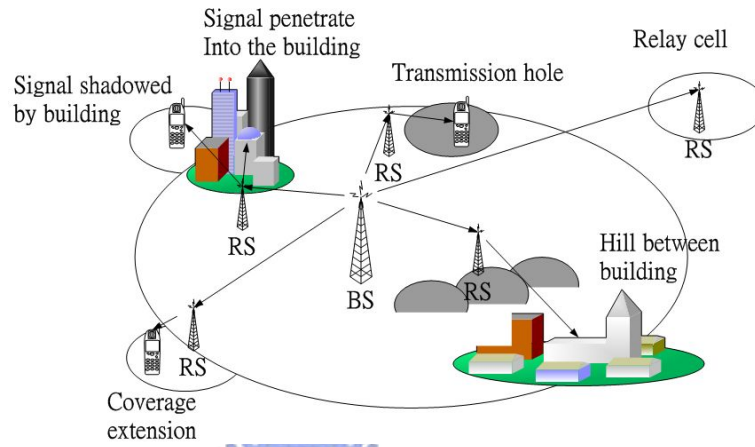
*Fig. 2.2:* Fixed Infrastructure Usage Model
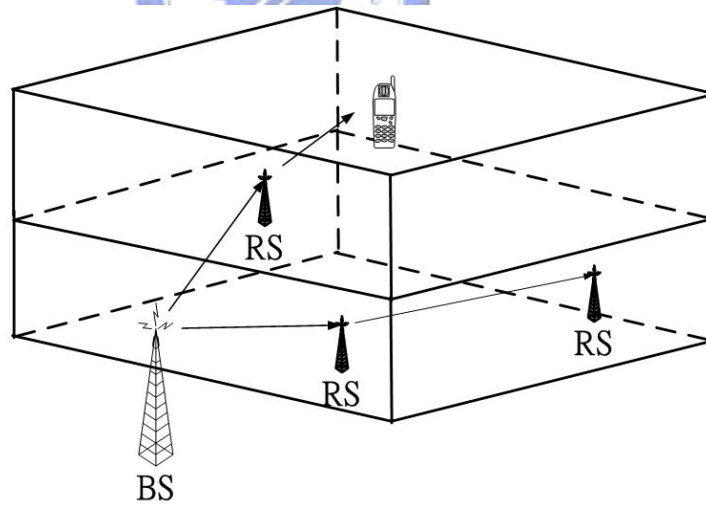


*Fig. 2.3:* In-Building Coverage Usage Model
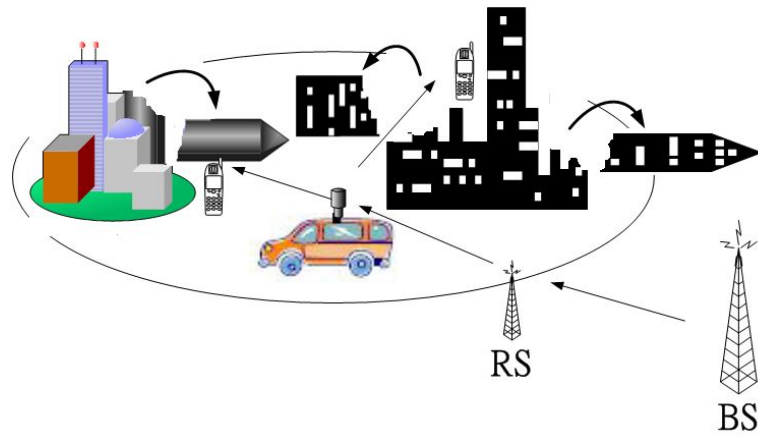
Fig. 2.4: Temporary Coverage Usage Model
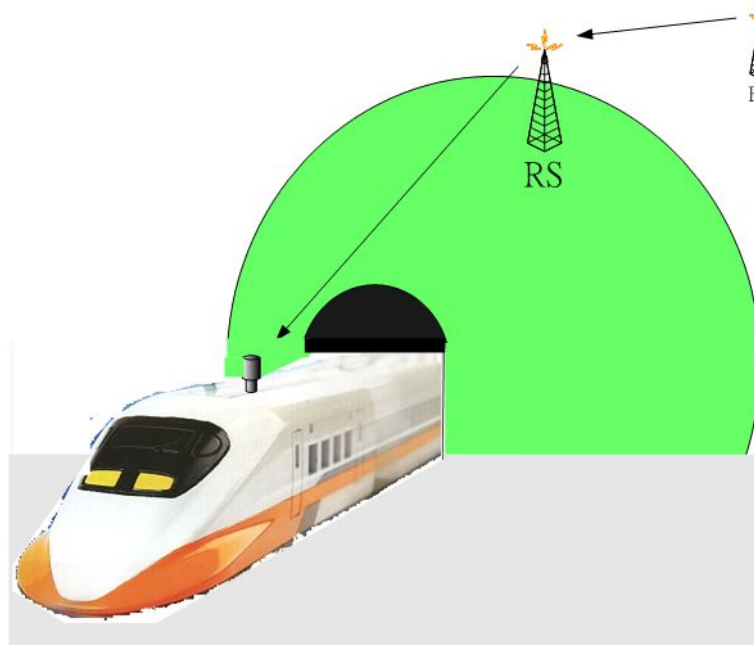


Fig. 2.5: Coverage on Mobile Vehicle Usage Model

# 2.3 Handoff Procedure in IEEE 802.16j Multi-Hop Relay Network

The IEEE 802.16j is a extend specification of IEEE 802.16e. The handoff procedure of IEEE 802.16j is based on that of IEEE 802.16e basically, but includes several new scenarios. The common processes of handoff include two stages: network topology acquisition and handoff process execution.

First, in topology acquisition stage, a MR-BS shall broadcast information about the network topology using the MOB_NBR-ADV message at a periodic interval. The message provides channel information for neighboring BS. A serving BS may obtain that information over the backbone. This information is very important for a MS to synchronize with neighboring BS while MS needs to handoff, it saving the bandwidth and time to monitor transmission of message from the neighboring BS. A BS will allocate time intervals to MS, which used to seeking neighboring BS and making handoff target decision. These time intervals is called the scanning interval.

Second, the handoff process is executed in which an MS decide to change the serving BS. The handoff process consists of the following stages: cell reselection, handoff decision and initiation, synchronization to target BS downlink, Ranging, termination of MS context and handoff cancellation. In the cell reselection stage, an MS scan BSs in order to determine the most suitable target station. The candidate BSs are listed in MOB_NBR-ADV message. Then, the serving BS will allocate scanning intervals to MS for cell selection. The more detail processes are described in the reference [3] Section 6.3.22.

The reference [7] described seven handoff scenarios of IEEE 802.16j network, see Fig. 2.6. An MR-BS owns all the information of associate RSs. These information is encapsulated in MOB_NBR-ADV control message, MR-BS broadcast this message
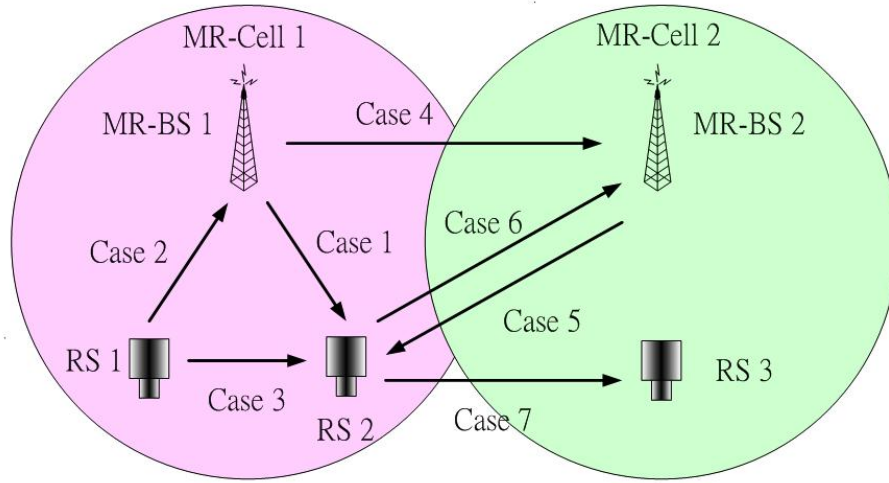
*Fig. 2.6:* Seven handoff cases in an relay network.

periodically [8]. Each relay link between MR-BS and RS is identified by primary CID, MOB_NBR-ADV message will be delivered hop by hop to every associate RSs. Finally, RS broadcast message to its MSs, see the Fig. 2.7 and Fig. 2.8.

For handoff process execution stage, the selected target station may request the MS information to speed up the process. According to the seven handoff scenarios as mentioned before, MS information may need to delivered over the relay link or wired backbone. Two new MAC management messages MS_INFO-REQ and MS_INFO-RSP were defined in the reference [9] to support the request of target station, see Fig. 2.9.

The handoff process can be categorized into two kinds: intra MR-BS handover and inter MR-BS handover:

1. Intra MR-BS handoff

    The target station is in the original MR-BS's cell. The MS information just needs to delivered over relay link. The signaling overhead is a little bit increased.
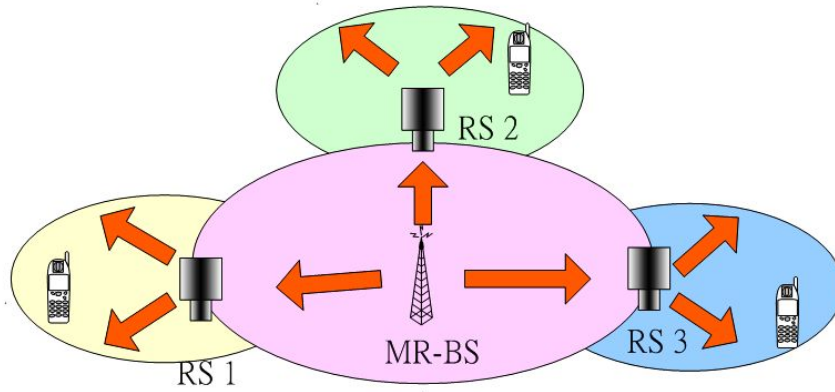
*Fig. 2.7:* Network topology advertisement in IEEE 802.16j
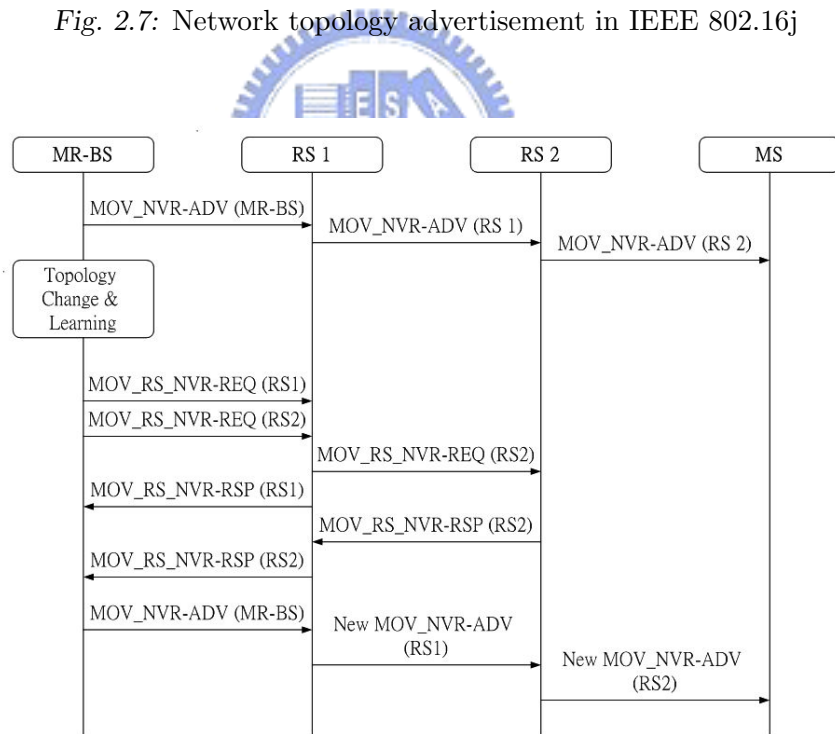


*Fig. 2.8:* Message flow of MOB_NBR-ADV transmission
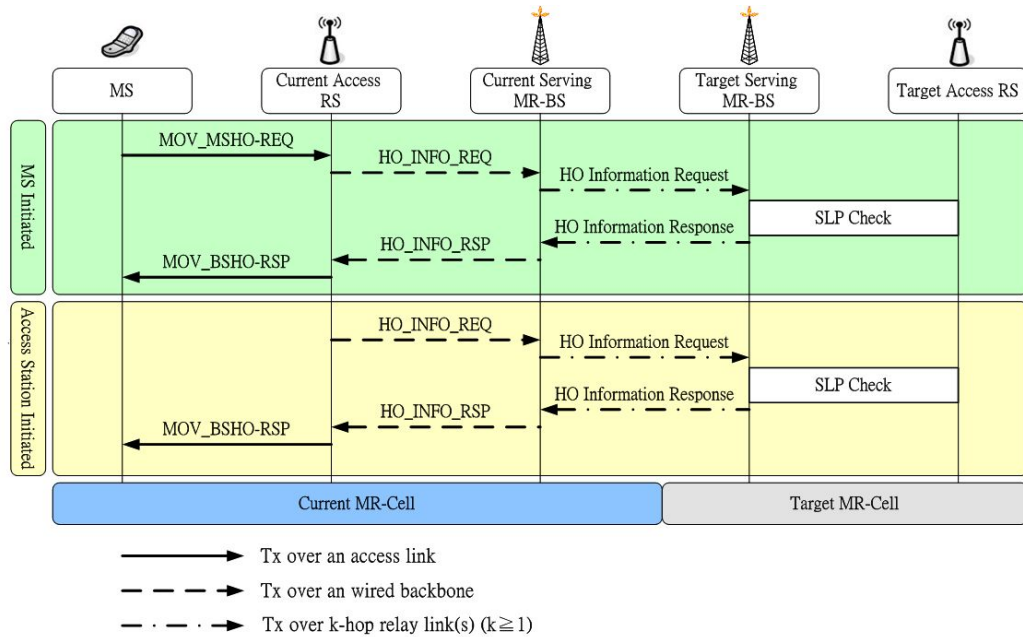
*Fig. 2.9:* Handoff Initiation in IEEE 802.16j.

2. Inter MR-BS handoff

   The target station is located in the neighboring MR-BS's cell, the MS information must delivered over wired backbone. The target station has to issue MS_INFO-REQ and MS_INFO-RSP over the relay links and/or over the wired backbone to request the MS information. The signaling overhead may be increased rapidly.

   The rest stages of handoff are described in the references [7] [10] [11] [9] [12] [13], and the more detail statements are listed in IEEE 802.16's Relay Task Group.
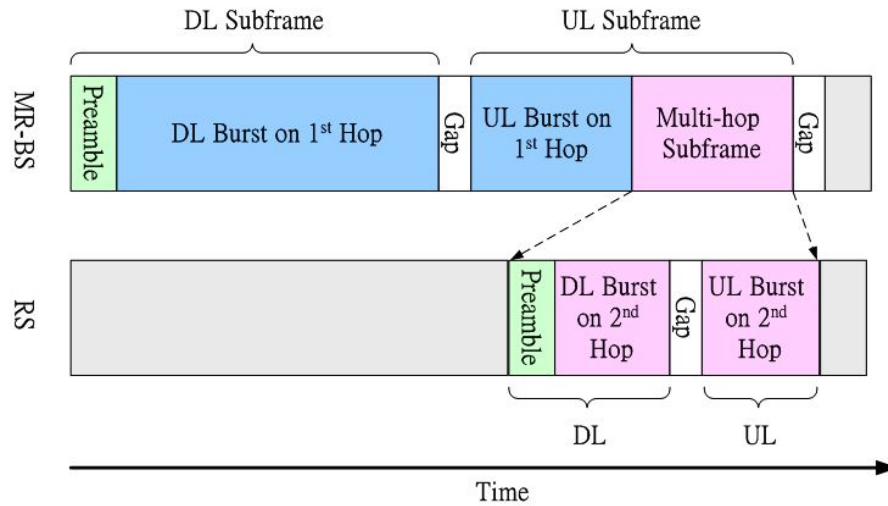
*Fig. 2.10:* The Suggested Frame Structure for IEEE 802.16j.

## 2.4 Frame Structure of IEEE 802.16j OFDMA Air Interface

The IEEE 802.16j standard inherents physical layer specification from IEEE 802.16e air interface. The network topology is mainly a tree-based architecture which constructed by MR-BS and RSs. An RS recieved signal from one hop (MR-BS or RS), then decode and forward to another hop (MR-BS, RS, or associate MS).

A new frame structure must be provided to support the requirement of signal relaying in the tree-based architecture. Fig. 2.10 shows a suggested frame structure [14]. During the multi-hop subframe interval, the BS does not schedule DL and UL traffic. Instead, RS fully control the assigned frame interval, and encapsulate MAC-layer control message in the frame. This frame is called multi-hop subframe. BS schedule a downlink time zone for RS, then RS can transmit its own frame to the next hop or associated MS.

Fig. 2.11: Frame structure for non-transparent mode.

The multi-hop subframe includes DL subframe and UL subframe. The DL subframe composed of the preamble and DL data burst. The DL data burst contain the MAC-layer control message. The UL subframe starts with a contention interval after DL data burst. MS use this interval for network entry or issues request for bandwidth adaptation.

In the reference [15], it proposes a frame structure with similar concept, see Fig. 2.11. In this design, the RS's operation is classified into two modes: transparent mode and non-transparent mode. For transparent mode, RS does not transmit its

own preamble. Thus, the RS's operation is fully controlled by the MR-BS, which include control message generation and frame interval scheduling. For non-transparent mode, an RS transmits its own broadcast preamble, FCH, DL-MAP/UL-MAP and DCD/UCD. Each RS is well aware of neighboring station, and it broadcast individual MOB_NBR-ADV message for its service area. In this thesis, we focus on the non-transparent mode.

## 2.5 OFDMA Subcarrier Allocations in Downlink Subframe

The first symbol of DL subframe is the preamble, and the preamble is modulated using BPSK modulation with well defined pseudo-noise (PN) code [3]. There are three types of preamble carriersets which differ from the allocation of different subcarriers to each other. Assume the FFT size is 1024, the preamble carriersets are defined as (2.1):

$$PreambleCarrierSet_n = n + 3k \tag{2.1}$$

where:

$PreambleCarrierSet_n$ : $specifies\ all\ subcarriers\ allocated\ to\ the\ specific$
$\qquad\qquad\qquad\qquad\quad preamble,$
$n$ : $is\ the\ number\ of\ the\ preamble\ carrier\ set\ indexed$
$\qquad\qquad\qquad 0...2,$
$k$ : $is\ a\ running\ index\ 0...284.$

The PN sequence of IEEE 802.16e OFDMA air interface is defined in the reference [2] [3] Table 309. The value of defined sequence shall be converted (0 mapped to +1 and 1 mapped to -1) from most significant bit (MSB) to least significant bit (LSB), then mapped into the subcarriers. It has to reserve 86 guard band subcarriers
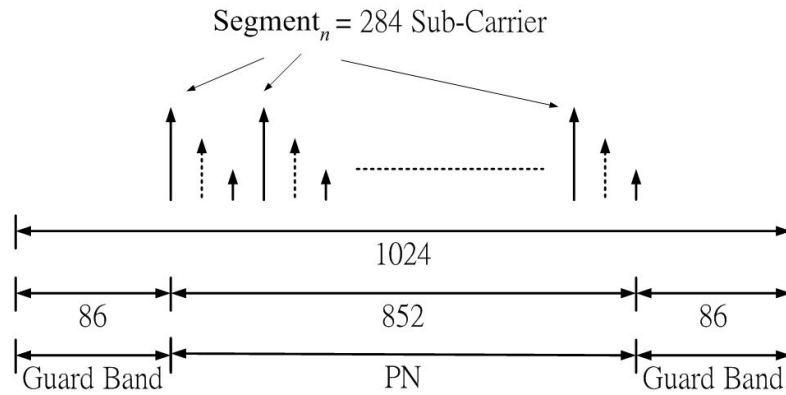
*Fig. 2.12:* The preamble structure of IEEE 802.16j OFDMA 1024 FFT points air interface.

on the left side and the right side of the spectrum. One example of 1024 FFT points preamble is shown in Fig. 2.12.

## 2.6   Channel Model

An important technique to evaluate the performance of a wireless system is to transmit signals into wireless channel. The wireless channel model should construct the path loss model, multipath delay spread model, fading characteristics, doppler spread, co-channel and adjacent channel interference, etc. Since different architecture of wireless system has different channel characteristics, thus different channel model should mapping to each usage scenario.

The IEEE 802.16 task group suggested two types of usage scenario: suburban and urban. For suburban, the channel model is based on the Hata-Okumura model and its extension [16] [17] [18] [19]. It is categorized into three types: category A, category B and category C for different path loss categories. The basic path loss formula is:

$$PL = A + 10\gamma log_{10}^{(d/d_0)} + s \tag{2.2}$$

where $A = 20log_{10}^{(4\pi d_0/\lambda)}$ ($\lambda$ being the wavelength in meter), $\gamma$ is the path-loss exponent with $\gamma = (a - bh_b + c/h_b)$ for $h_b$ between $10m$ and $80m$ ($h_b$ is the height of the base station in meter), $d_0 = 100m$ and $a$, $b$, $c$ are constants dependent on the category.

We can adjust the configuration of channel model for other frequencies and for receive antenna heights between $2m$ and $10m$. The modified path loss model would be:

$$PL_{modified} = PL + \triangle PL_f + \triangle PL_h \qquad (2.3)$$

where $PL$ is the path loss given in equation 2.2, $\triangle PL_f$(in dB) is the frequency correction term, given by

$$\triangle PL_f = 6log_{10}^{f/2000}$$

where $f$ is the frequency in $MHz$, and $\triangle PL_h$ is the receive antenna height correction term given by:

$$\triangle PL_h = -10.8 \cdot log_{10}^{(h/2)} \quad , Categories \, A \, and \, B$$

$$\triangle PL_h = -20 \cdot log_{10}^{(h/2)} \qquad , Categories \, C$$

where $h$ is the receive antenna height between $2m$ and $10m$.

For urban, Cost 231 Walfish-Ikegami (W-I) model is used to describe the channel model with uniform building height. In this model, the path loss effect is influenced by three factors:

$$L_b = L_0 + L_{rts} + L_{msd}$$

where $L_0$ is free space loss, $L_{rts}$ is roof top to street diffraction and $L_{msd}$ is multi-screen loss. The detail can be seen in the reference [20].

In IEEE 802.16j network, the Stanford University Interim (SUI) channel models [21] is adopted to describe the channel characteristics. SUI model gives a general
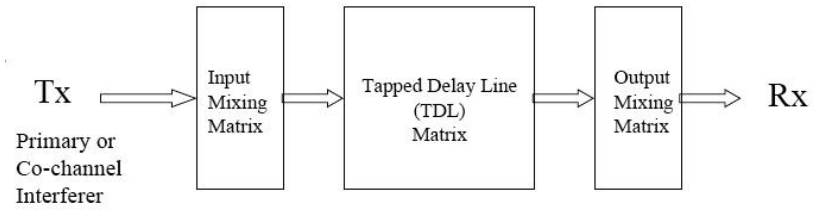
*Fig. 2.13:* The channel structure of SUI channel model.

form to include possible combinations of parameters to obtain channel descriptions. SUI model combines all parameters which are mentioned before, and make a mapping to different usage models. The general structure of SUI channel model show in the Figure 2.13 and the detail can be seen in [22].

# CHAPTER 3

# Frame Arrival Detection and Estimation of FFT Size and CP Length

## 3.1 Introduction

In this chapter, we investigate how to detect the frame arrival event with obtaining FFT size and CP length. The synchronization process usually includes two steps: coarse synchronization and fine synchronization. Frame arrival detection belongs to coarse synchronization which used to detect whether a frame is coming. The fine synchronization mainly estimates the frame starting time. As mentioned before, our goal is to estimate the difference of frame inter-arrival time, which is used for best target selection. To achieve this goal, frame arrival detection must be accomplished first.

Traditionally, frame arrival detection is implemented by the auto-correlation

of the predefined preamble. A receiver must know the information of FFT size and CP length before it starts to execute synchronization process. If it doesn't know the FFT size, it will not know when to stop the frame arrival detection process. If it doesn't know the CP length, it will not know how long a symbol period must be deleted before sending signal into FFT block. Usually, FFT size and CP length are known from the upper layer MAC message.

In our considered case (wireless multi-hop relay networks), an MS needs to compare the difference of frame inter-arrival time from different RSs or BSs to select the most suitable handoff target. Since the target RS or BS has not been decide yet, and system control message may not received from BS, FFT size and CP length of candidate target stations may not be obtained by the MS. Furthermore, the FFT size and CP length are variable in OFDMA-based WiMAX systems. Thus, the frame arrival detection is required to perform without information of FFT size and CP length.

We develop a fast PHY layer solution to estimate FFT size and CP length without depending on any MAC-layer message. This technique help to accomplish the synchronization process more quickly.

The rest of this chapter is organized as follows. In Section II, we describe the system model. In Section III, we discuss the problem of frame arrival detection. In Section IV, we provide frame arrival detection and FFT estimation algorithm which based on the conjugated symmetric characteristic of BPSK modulated preamble. In Section V, we discuss the CP length. In Section VI, we define the performance evaluation metrics, and show the simulation results to compare the proposed algorithm with conventional algorithm under different channel model and give concluding remarks in Section VII.

## 3.2   System Model

We consider an $N$ FFT points OFDM system with one transmit antenna and one receive antenna. The total bandwidth of each subchannel is assumed to be smaller than the channel coherent bandwidth.

      The FFT-based technique are typically employed in the baseband OFDM modulation/demodulation process as Fig. 3.1. The serial data stream is split to parallel data stream with a data rate of $1/T_{sym}$, which $T_{sym}$ is symbol duration. The resulting symbol stream is modulated into a vector of $N$ data symbol $X[0]$ to $X[N-1]$. The inverse FFT (IFFT) of the data symbol vector $x[0]$ to $x[N-1]$ transfer symbol from frequency domain to time domain, this is called the subcarrier. Thus the $x[n]$ are the time domain samples of the OFDM symbol and transmitted sequentially over the channel.

      A low complexity technique of preventing the interference of transmitted consecutive OFDM symbols is to copying a short period of symbol from the symbol tail and adding it to the front of symbol. It is assumed that the CP length is greater than the length of the discrete-time baseband channel impulse response so that the frequency-selective fading channel decouples into a set of parallel frequency-flat fading channels [23]. Denoting the transmit and receive signal vectors with $\mathbf{x}_n$ and $\mathbf{y}_n$ respectively. We can write:

$$\mathbf{r}_k = \mathbf{H}_k \mathbf{s}_k + \mathbf{w}_k \tag{3.1}$$

where $k$ is the subcarrier index and $\mathbf{H}_k$ represents the channel matrix of the $k$-th subcarrier. Here, each entry of $\mathbf{H}_k$ is an i.i.d. circular-symmetric complex Gaussian variable [24]. $\mathbf{w}_k$ represents the white noise vector with $E[\mathbf{w}_k \mathbf{w}_k^*] = \sigma_k^2 \mathbf{I}$ where $*$ is the transpose conjugate operation. We assume all subcarriers experience the same frequency shift and the equally spaced samples of the received signal contain an
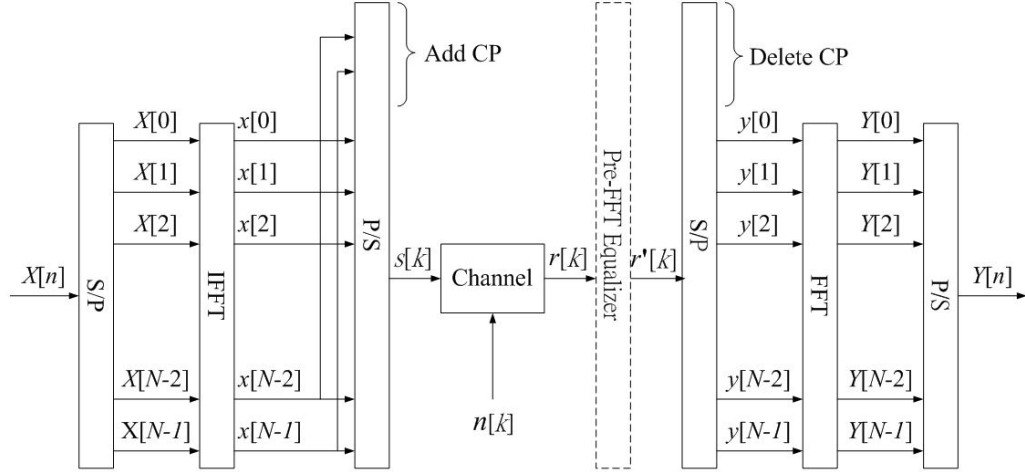
*Fig. 3.1:* The system model of $N$-subcarrier OFDM transmission system.

unknown starting time. Thus the form of received signal can be represented as the following:

$$s[k] = \frac{1}{\sqrt{N}} \sum_{n=0}^{N-1} x[n] e^{j\frac{2\pi}{N}nk}, \quad -N_{cp} \leq k \leq N-1 \tag{3.2}$$

$$r[k] = \sum_{\ell=0}^{L-1} h(\ell) s(k-\ell) + n[k] \tag{3.3}$$
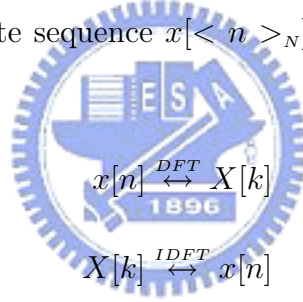
which $L$ is channel length.

The pre-FFT equalizer is used to deal with the time-dispersive effect. Though OFDM is a novel technology to overcome ISI, but the multi-path effect caused by building in the urban environment still cause timing offset and lead to the overlap of signal. This will seriously influence synchronization performance. We have to re-correct the signal before input into FFT block.

## 3.3 Conjugated Symmetric Characteristics of BPSK Modulated Preamble

OFDMA-based air interface of IEEE 802.16 standard is defined in [2] [3]. The frame arrival detection is accomplished by making auto-correlation of preamble. The most important things of synchronize is knowing PHY information, such as CP length, FFT size and accurate frame arrival time. Here, we firstly prove that BPSK modulated preamble has special characteristics by Fourier transform, these characteristics will be the basis to estimate the PHY information.

The discrete-time Fourier transform (DFT) shows good properties in signal transformation. For a finite sequence $x[<n>_N]$ with length $N$, define the Fourier transform pair:

$$x[n] \overset{DFT}{\leftrightarrow} X[k]$$

$$X[k] \overset{IDFT}{\leftrightarrow} x[n]$$

its *circular reverse time-shefting* can be represented as:

$$x[n] = \begin{cases} x[N-n] & ,0 \le n \le N-1 \\ x[n] & ,n=0 \end{cases}$$

If a complex sequence with length $N$ satisfied following equation:

$$x[n] = x^*[-n] = x^*[N-n], \quad 0 \le n \le N-1$$

it called the *circular conjugate-symmetric*. Then, define

$$x[n] = x_{cs}[n] + x_{ca}[n], \quad 0 \le n \le N-1 \ . \tag{3.4}$$

where

$$x_{cs}[n] = \frac{1}{2}(x[n] + x^*[-n]), \quad 0 \le n \le N-1$$

$$x_{ca}[n] = \frac{1}{2}(x[n] - x^*[-n]), \quad 0 \le n \le N-1$$

which $x_{cs}[n]$ represents *the circular conjugate-symmetric part* and $x_{ca}[n]$ represents *the circular conjugate-antisymmetric part.* Usually the DFT of $x[n]$, is a complex sequence, it can be represented as following:

$$X[k] = X_{Re}[k] + jX_{Im}[k]$$

then

$$
\begin{aligned}
X[k] &= \sum_{n=0}^{N-1}(x_{Re}[n] + jx_{Im}[n])(\cos(\frac{2\pi nk}{N}) - j\sin(\frac{2\pi nk}{N})) \\
&= \underbrace{\sum_{n=0}^{N-1}(x_{Re}[n]\cos(\frac{2\pi nk}{N}) + x_{Im}[n]\sin(\frac{2\pi nk}{N}))}_{X_{Re}[k]} + \\
&\quad j \cdot \underbrace{\sum_{n=0}^{N-1}(x_{Im}[n]\cos(\frac{2\pi nk}{N}) - x_{Re}[n]\sin(\frac{2\pi nk}{N}))}_{X_{Im}[k]}
\end{aligned}
$$

assume $X[k] \in \mathbf{R}$ are real values, we can get that:

$$X_{Re}[k] = \frac{1}{2}(X[k] + X^*[k])$$

and

$$X^*[k] = \sum_{n=0}^{N-1} x^*[n]e^{j2\pi nk/N}$$

$$= \sum_{n=0}^{N-1} x^*[N-n]e^{j2\pi(N-n)k/N}$$

$$= \sum_{n=0}^{N-1} x^*[N-n]e^{-j2\pi nk/N} \tag{3.5}$$

thus

$$X^*[k] \overset{IDFT}{\leftrightarrow} x^*[N-n]$$

so we can get

$$X_{Re}[k] \overset{IDFT}{\leftrightarrow} \frac{1}{2}(x[n] + x^*[N-n]) = x_{cs}[n] \tag{3.6}$$

this means if a finite sequence is real value in frequency domain, its inverse discrete Fourier transform (IDFT) sequence will be circular conjugate-symmetric. In our system model, the BPSK modulated preamble is a sequence $X[k]$ in frequency domain. After passing through the IDFT block, the $X[k]$ are transformed into time domain complex signal, and it has the characteristic of circular conjugate-symmetric.

It's true that $x[n]$ is circular conjugate-symmetric since the BPSK modulated preamble is real number. In our system model, the result can be concluded as follow equation:

$$s[k] = s^*[N-k] \tag{3.7}$$

After passing through IDFT block, a copy of the tail of the useful symbol period (i.e CP), the whole preamble symbol forms two symmetric characteristics as shown in Fig.3.2:
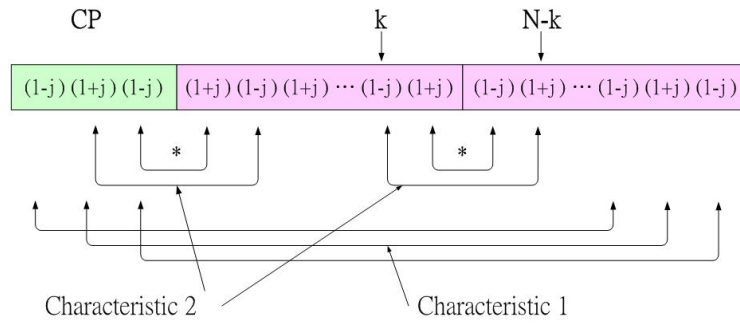
*Fig. 3.2:* Symmetric characteristics of BPSK modulated preamble after discrete-time fourier transform.
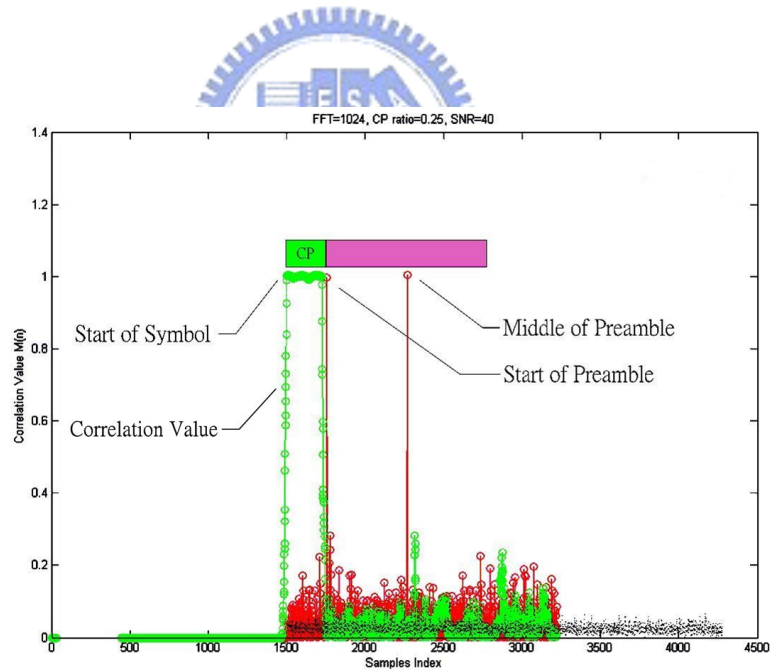


*Fig. 3.3:* Correlation value of symmetric characteristics of BPSK modulated preamble.

1. Characteristic 1:

   Since the CP is copied from the tail of the preamble, we can make auto-correlation between CP and the tail of preamble symbol. This can be used to frame arrival detection, FFT size estimation and CP length estimation.

2. Characteristic 2:

   This characteristic appears at two position. The first is located on the tail of CP and the front of the preamble. The second is located on the middle of the preamble symbol. The first one is the starting point of preamble. We can reverse the order of signal in the first part of these two symmetric signals, then making correlation. The correlation value will show two peaks, the first peak is the starting point of preamble symbol.

   In this thesis, we will be fully utilized these two characteristics to accomplish frame arrival detection and frame arrival time estimation. After these two processes, a receiver can locate accurate time domain preamble starting point. The preamble position and the measurable metrics can be concluded in Fig. 3.3.

## 3.4 Proposed Frame Arrival Detection and FFT Sizes Estimation Algorithms

The first stage to execute synchronization is to detect the frame arrival event, then the receiver can configure itself to receive framing signal. In the IEEE 802.16e OFDMA air interface (which followed by IEEE 802.16j network) defines four cyclic prefix ratio: 1/4, 1/8, 1/16, 1/32. Once MS receives signal frames from candidate target stations, it has to analyze the FFT size and CP length of each frame.

   We discuss the traditional algorithm of frame arrival detection first. In the reference [25], the basic concept of algorithm is to transmit two repetitive training
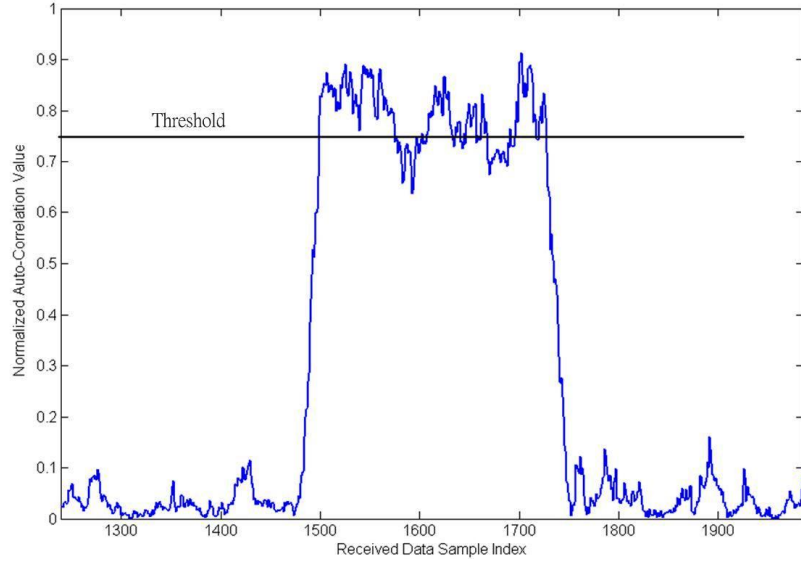
*Fig. 3.4:* The auto-correlation value and threshold to detect frame arrival event.

sequences, and make auto-correlation at the receiver side:

$$P[k] = \sum_{m=0}^{L-1}(r[k+m]^* \cdot r[k+m+d]), \quad R[k] = \sum_{m=0}^{L-1}|r[k+m+d]|^2,$$

$$M[k] = \frac{|P[k]|^2}{(R[k])^2} \ . \tag{3.8}$$

which $L$ is correlation windows length, and $d$ is correlation delay. If the correlation value higher than predefined threshold, the receiver trigger a frame arrival event. The result of auto-correlation value and threshold are shown in Fig. 3.4.

This solution has some disadvantages :(1) it could just detect frame arrival event, but not estimating FFT size and CP length; (2) in low SNR area, it tends to trigger the false alarm frequently owing to the unstableness of auto-correlation value; (3) because of the unstableness of auto-correlation value, it's difficult to determine the threshold.

To improve reference [25], we provide a robust frame arrival detection algo-
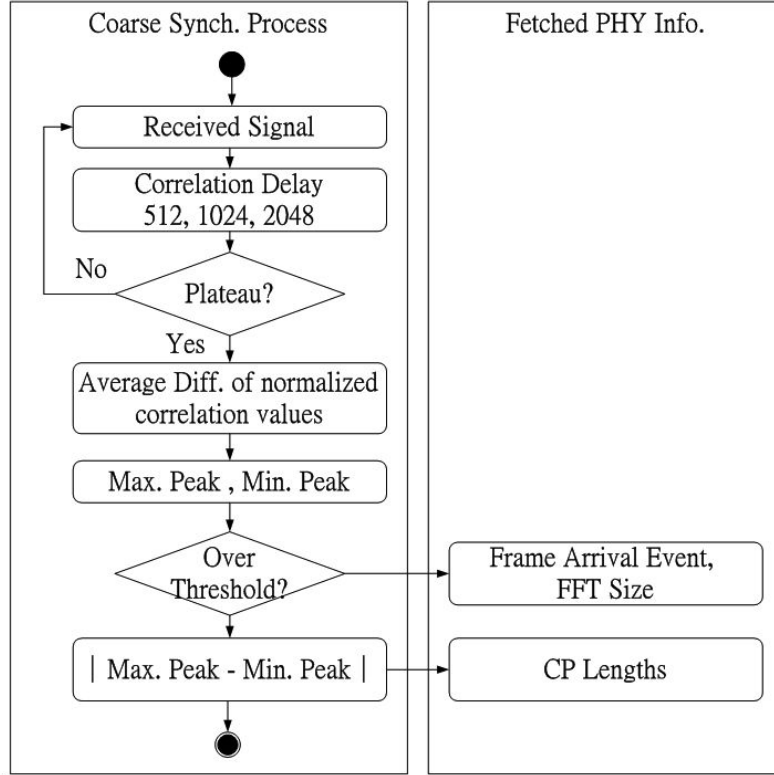
*Fig. 3.5:* Proposed algorithm of frame arrival detection, FFT size estimation and CP length estimation.

rithm which based on the average difference of normalized auto-correlation values, see Fig. 3.5. This algorithm will not only improve the performance of frame detection, but make it possible to detect the FFT size and CP length. First, we adopt the symmetric characteristic 1, then make auto-correlation between CP and the signals behind specify correlation delay $d$ ($d = 128, 512, 1024, 2048$). Second, finding the difference between one point and its later mean normalized values, this can measure the changing rate of correlation value:

$$M^{'}[k] = \frac{\sum_{l=0}^{S-1} M[k+l]}{S} - M[k] \qquad (3.9)$$
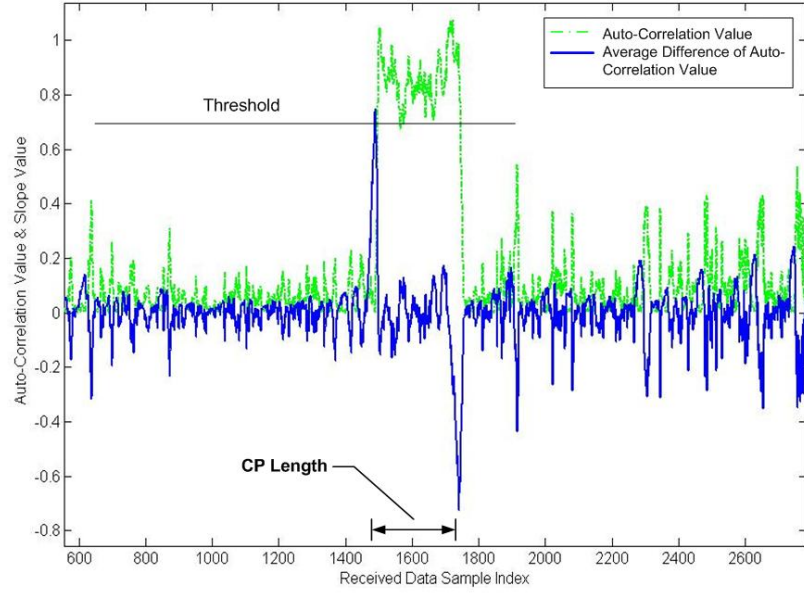
*Fig. 3.6:* The average difference of auto-correlation value for frame arrival detection and CP length estimation.

where $S$ is the sample number that we take average. Once the specific correlation delay $d$ equals to the FFT size of preamble, a plateau of auto-correlation values will be appear. Then, we calculate the difference of normalized auto-correlation values, there will be two peaks, see Fig. 3.6.

Since it monitors the changing rate of auto-correlation value, it is more sensitive on detecting frame arrival event than the algorithm proposed in the reference [25]. If the max. peak is higher than the given threshold (here, threshold=0.7), the frame arrival event and FFT size can be determined.

The performance metrics of frame arrival detection can be represented as the correct probability of frame arrival event. The alert is true if the value of max. peak is higher than the specific threshold, and the sampling index is located on the edge of plateau of correlation values. Thus, we can compare performance between the

reference [25] and the proposed algorithm.

## 3.5    Proposed CP Length Estimation Algorithm

According to the definition of OFDMA in the references [2] [3], there are four types of CP ratio: 1/4, 1/8, 1/16, 1/32. Using a cyclic extension, the samples required for performing the FFT at the receiver can be taken anywhere over the cyclic prefix. This provides multipath immunity as well as a tolerance for symbol time synchronization errors.

According to [2] [3], an MS should search all possible lengths of CP until it finds real CP length being adopted by BS on initialization. The MS shall use the same CP on the uplink transmission. Once a specific CP length has been determined by the BS for operation on the downlink, it should not be changed. Changing the CP would force all the MSs to re-synchronize to the BS.

In this thesis, we assume the MS moving in the metropolitan area. An MS may encountered many signal frame with different CP length and different FFT size. An MS needs a new approach to detect these information more efficiently. Without these information, MS could not finish synchronization process within one symbol duration. This may cause the retransmission of upper layer MAC message, then the throughput may decreased.

Here, we continue using the concept which mentioned in prior section to solve this issue. From Fig. 3.6, we can see that there are two peaks which represents the beginning edge and the end edge of the CP. We provide a simple mathematical equation to detect CP ratio $\gamma$ and CP length $L_{cp}$:

$$\gamma \quad = \quad \underset{2 \leq i \leq 5}{\arg} \ min\{|t_{max} - t_{min}| - \frac{N}{2^i}\}$$

$$L_{cp} \quad = \quad \frac{N}{2^\gamma} \tag{3.10}$$
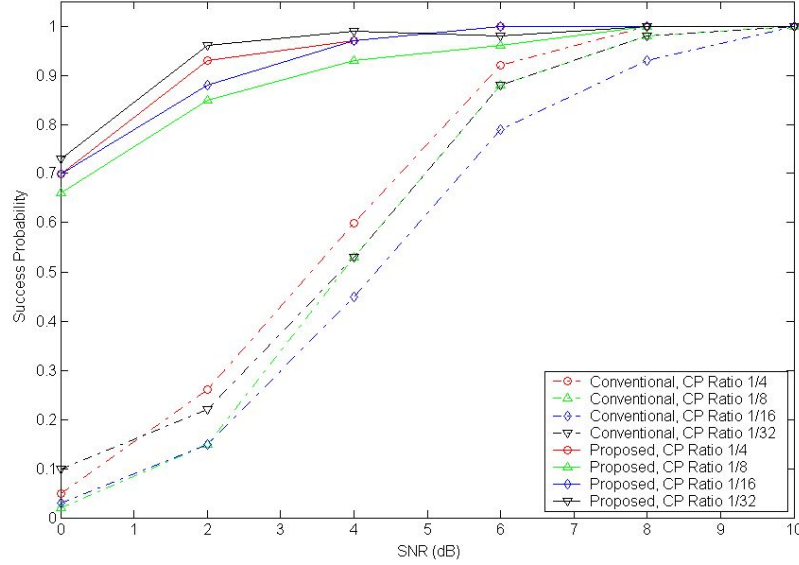
*Fig. 3.7:* The comparison of successful probability of frame arrival detection under AWGN channel.

where $t_{max}$ is the sampling time index of the maximum peak, $t_{min}$ is the sampling time index of the minimum peak, and $N$ is the estimated FFT size of preamble.

## 3.6   Simulation Results

The performance comparison of frame arrival detection under AWGN channel is shown in Fig. 3.7 with different CP ratio. We can see that the larger the CP ratio is, the higher the successful probability. The proposed algorithm works better than that in the reference [25] at low SNR area, and both of them limit to 1 after $SNR > 10(dB)$.

The performance comparison of frame arrival detection under SUI-3 channel is shown in Fig. 3.8 with different CP ratio. The proposed algorithm are still better than that in the reference [25] at low SNR area. But, since SUI-3 is a time-dispersive
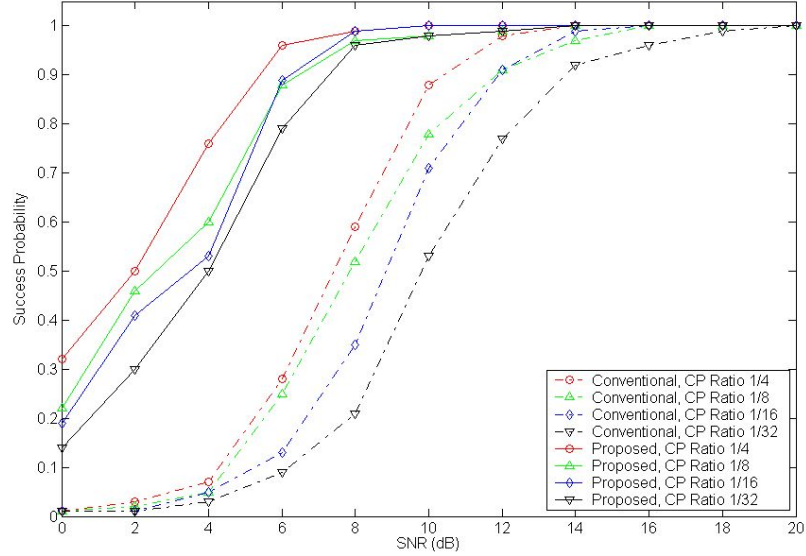
*Fig. 3.8:* The comparison of successful probability of frame arrival detection under SUI-3 channel.

channel, both of them are worse than that under AWGN channel.

The successful probability of FFT size estimation is depending on frame arrival detection. We can refer to Fig. 3.7 and Fig. 3.8. Since the reference [25] can not estimate CP length, we just compare the proposed algorithm under AWGN and SUI-3 channel, as show in Fig. 3.9. The result shows that when the CP length is getting larger, the successful probability is getting higher. It's is no doubt that the performance under AWGN channel is better than that under SUI-3 channel. The successful probability coming close to 1 when SNR is larger than $10\,dB$.

This approach can help MS detecting the CP length of symbol which transmitted by different candidate target station efficiently, and BS could adjust its CP ratio in each frame dynamically to adapt the change of link quality.
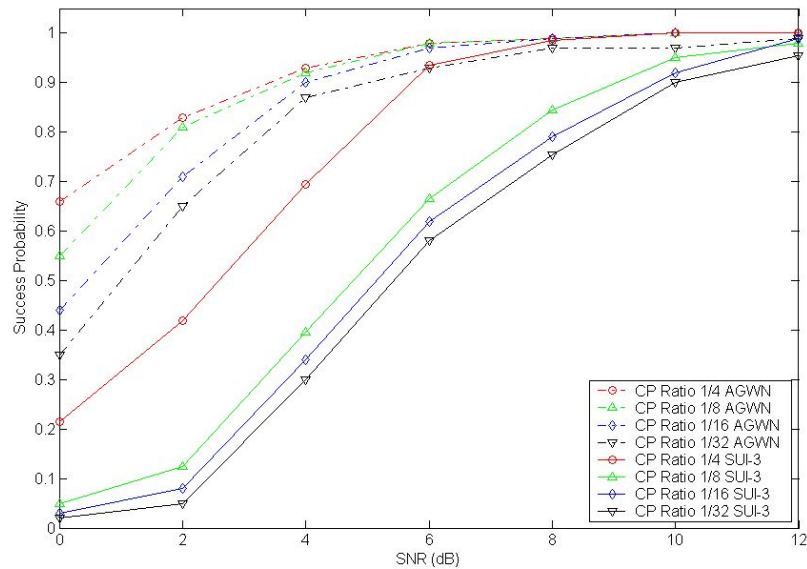
*Fig. 3.9:* The comparison of successful probability of cyclic prefix (CP) ratio under AWGN
and SUI-3.
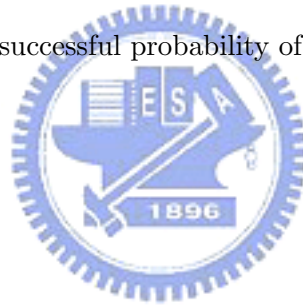
## 3.7   Conclusion

In this chapter, we fully utilize the symmetric characteristic 1 of BPSK modulated
preamble to accomplish frame arrival detection and FFT size estimation. By taking
the difference of normalized correlation value, successful probability for frame arrival
detection of proposed solution is better than conventional algorithm. Furthermore,
CP length can also be estimated well.

# CHAPTER 4

# Frame Arrival Time Estimation

## 4.1 Introduction

In this chapter, we investigate how to estimate frame arrival time. The frame arrival time estimation determine the accurate start point of a frame. This process also called the fine synchronization. We can estimate the frame duration by monitoring frame inter-arrival time. Thus, the difference of frame inter-arrival time between system predefined frame duration and observed frame duration can be estimated, which help for the best target selection.

Numerous frame arrival time estimation algorithms [25] [26] [27] [28] have been published so far. The conventional algorithms are usually achieved by making cross correlation between received signal and well defined PN sequence. In IEEE 802.16 network, an MS must get the preamble index from MAC message first, and then use this index to get the PN sequence from a predefined mapping table. This mechanism may seriously increase signaling overhead.

In our considered wireless multi-hop relay networks, an MS may not get the PN

sequence since the target station has not been selected yet. To estimate the difference of frame inter-arrival time, we proposed a pure PHY layer algorithm without obtaining predefined PN sequence.

The rest of this chapter is organized as follows. In Section II, we describe the system model. In Section III, we provide a CP-based frame arrival time estimation algorithm. In Section IV, we show the simulation results to compare the performance of proposed algorithm under different channel model and give concluding remarks in Section V.

## 4.2 System Model

We continually adopt the system model described in Chapter 3, and a pre-FFT equalizer is used to overcome time-dispersive effect of the channel while CP length is shorter than the length of transient response of the channel. Without this equalizer, any delayed finger will interfere with the original signal while pass through a time-dispersive channel such like SUI-3, and the frame arrival time estimation will be failed. Furthermore, BER will rise shapely after signal pass through FFT block and be decoded. Since the requirement of estimation precision is so serious, pre-FFT equalizer play a important role to receiver design.

The pre-FFT equalizer is to filter the received time spread signal adaptively before it input into FFT block. The basic concept is shown in Fig. 4.1, and the signal form is:

$$r_k = h_k \otimes s_k = \sum_i h_i \cdot s_{k-i} \tag{4.1}$$

from Fig. 4.1, the equalizer output is:

$$r_k^{'} = u_k \otimes r_k = u_k \otimes h_k \otimes s_k \tag{4.2}$$
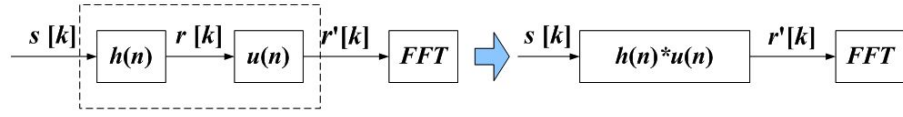
*Fig. 4.1:* Concept of pre-FFT equalizer.

## 4.3 Proposed CP-based Frame Arrival Time Estimation Algorithm

The conventional frame arrival time estimation algorithm is achieved by making cross correlation between received signal and well defined PN sequence. In IEEE 802.16j network, though MS could get preamble index from MOB_NBR-ADV message, and then search Table 309a to get PN sequence, but the MOB_NBR-ADV message broadcasting may seriously increase signaling overhead. But, for inter MR-BS handoff, RSs belongs to different MR-BS cell may not know each other, thus MOB_NBR-ADV message may not include this candidate target station.

We propose a simple algorithm based on the symmetric characteristic 2 of BPSK modulated preamble as described in Chapter 3. We reverse the received signal at the CP, and then make auto-correlation with conjugated rear signal:

$$P(n) = \sum_{i=0}^{L-1}(r'_{n-1-i} \cdot r'^{*}_{n+1+i}) \tag{4.3}$$

where $L$ is correlation windows, we set $L = 16$ here. If sampling time index $n$ going to the preamble starting time index, a perfect correlation peak should be appears.

We adopt the zero-forcing (ZF) algorithm to design our pre-FFT equalizer. We assume that receiver can make channel estimation by using pre-coded sequence which embedded in preamble [29] [30] [31], then make channel estimation by adopting the

least square (LS) algorithm to find out the channel vector (channel impulse response):

$$r_k = h_k \otimes s_k + w_k = Sh + W ,$$

$$h_{est} = (S^H S)^{-1} S^H r_k \tag{4.4}$$

The channel vector can be used to design the coefficient of equalizer, which is used for channel inversion. The channel vector can transfer to be a channel matrix:

$$H = \begin{bmatrix} h_{est}(1) & 0 & 0 & ... & 0 \\ h_{est}(2) & h_{est}(1) & 0 & ... & 0 \\ h_{est}(3) & h_{est}(2) & h_{est}(1) & ... & 0 \\ . & . & . & ... & . \\ . & . & . & ... & . \\ h_{est}(Q) & . & . & ... & h_{est}(1) \end{bmatrix}$$

which $Q$ is the length of pre-coded sequence. We pre-coding the first $Q$ samples of preamble to be the training sequence. Then we can get the coefficient of equalizer:

$$C = H^{-1} e_d^T \quad , \quad e_d^T = [0, ..., 1, ..., 0]^T \tag{4.5}$$

finally, the received signal passing through this equalizer before it input to the FFT block. The received signal becomes:

$$r_k' = \sum_{i=0}^{Q-1} C_{k+i} \cdot r_{k+i} \tag{4.6}$$

## 4.4 Simulation Result

The simulation result of frame arrival time estimation is shown in Fig. 4.2. Here, we define the success probability as that receiver can detect the time index of preamble starting time at the true location successfully. We compare the performance under
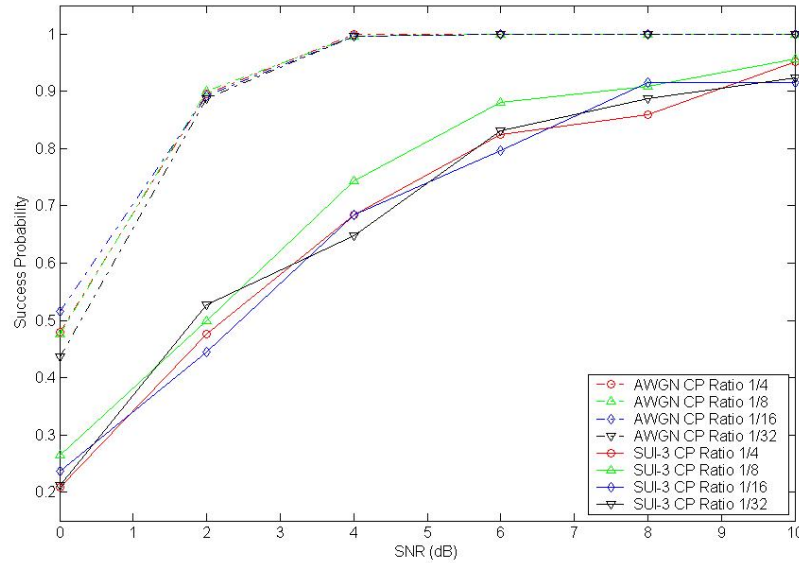
*Fig. 4.2:* The comparison of successful probability frame arrival time estimation under AWGN and SUI-3 channel.

AWGN and SUI-3 channel. We can find that no matter which CP ratio of preamble signal, the success probability are almost the same. Besides, since the zero forcing equalizer enlarge the noise when it make channel inversion, so its performance at low SNR is not so good, but still reliable under SUI-3 channel.

## 4.5 Conclusion

In this chapter, we propose a total solution to frame arrival time estimation. This can be accomplished by symmetric characteristics 2 of BPSK modulated preamble. We provide a pre-FFT equalizer to eliminate delay spread under time dispersive channel. According to the simulation results, we can proof that the proposed approach performs well.

In next chapter, we will propose a Time-of-Arrival based target selection algo-

rithm to reduce handoff events, which take advantage of relative movement indicator.

# CHAPTER 5

# Difference of Frame Inter-arrival Time Based Target Selection Scheme for Reducing Handoffs in Wireless Multi-hop Relay Networks

## 5.1 Introduction

We discuss how to estimate the difference between observed frame duration and system predefined frame duration in this chapter. The difference represents an MS's mobility pattern, and will be useful for making the most suitable decision of target selection in handoff.

The traditional target selection scheme of handoff only depends on RSSI. But

in a metropolitan environment, it will trigger lots of unnecessary handoff process since the signal strength is unstable which because of the signals shadowed by the building. Thus, a new target selection scheme is required.

We propose a target selection algorithm which based on the difference of frame inter-arrival time. We use the technique which described in the Chapter 3 and Chapter 4 to get the observed frame duration (i.e observed frame inter-arrival time), then make a comparison with predefined system frame duration. The difference between these two values represents the mobility pattern of an MS. We called this information the relative movement indicator (RMI). In addition to RSSI, RMI of MS is suggested to target station selection. With RMI, an MS can judge whether it is moving toward an RS/BS or leaving away an RS/BS. Thus, an MS can choose a target RS/BS which it moving toward directly. By doing this, the unnecessary handoff can be avoid.

The rest of this chapter is organized as follows. In Section II, we describe the system model, which including Manhattan-like urban model and path loss model. In Section III, we describe how to estimate the RMI. In Section IV, we propose a time-of-arrival based target selection algorithm. In Section V, we show the simulation results to see the performance of reducing handoffs and give concluding remarks in Section VI.

## 5.2 System model

### 5.2.1 Manhattan-like Urban Model

To simulate the metropolitan environment, we design a simulator of Manhattan-like urban environments. we reference to the grid design of [32] [33], and the relative parameter setting are shown in the Table 5.1.

ART means the antenna is above roof top, and BRT means the antenna is

| Parameter | Value |
|---|---|
| Building Block Width | 200 meters |
| Road Width | 30 meters |
| Frequency Reuse Factor | 1 |
| RS Deployment Model | Uniform and non-uniform distribution |
| Antenna Height | ART or BRT |

*Tab. 5.1:* Manhattan-like urban model

below roof top. Uniform distribution of RS means every intersection of street has one target station, and non-uniform distribution means some intersection do not deploy RS.

## 5.2.2   Path Loss Model

In the urban area, building block heavily influence the signal transmission. But if the distance between target station and MS is very close and nothing located between them, the transmission path could be treated as LOS path. In the reference [34], it captures scope of the 802.16j multi-hop system evaluation methodology including the path loss model, traffic model and performance metrics. The path loss for the IEEE 802.16j contains the basic models from the IEEE 802.16-2004 and additional four path-loss model associated with RS.

We include three path loss model except Type-G, and concluded these models in the Table 5.2. This table also mapping the usage model and the path loss model to construct a evaluation configuration. The detail mapping result relative to the MS is listed in the reference [34] Table 2.

For Type-E case, the main feature is one node's antenna is ART, and the other

(a) Uniform deployment          (b) Non-uniform deployment
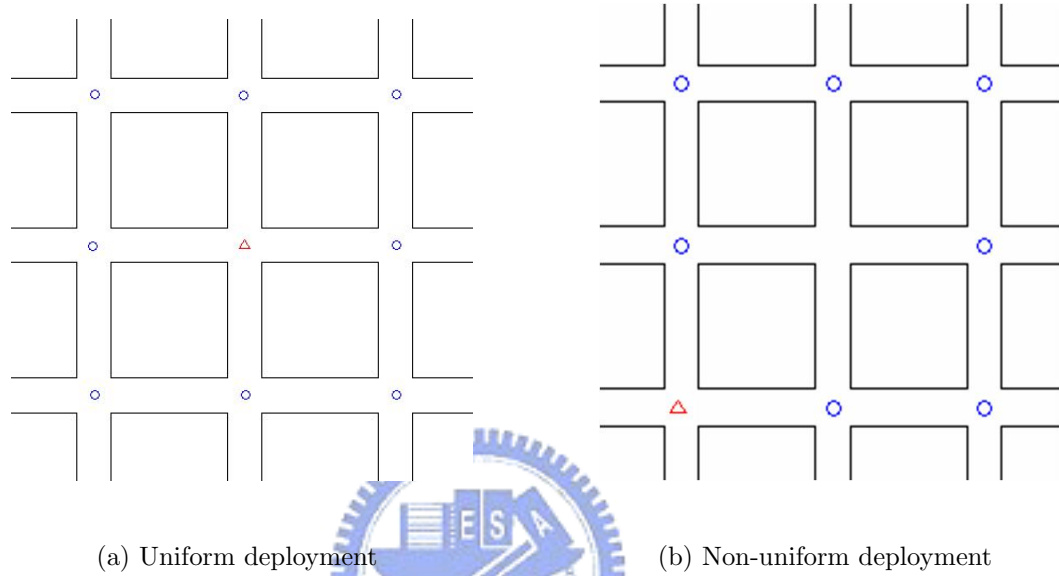
*Fig. 5.1:* Two deployment model of RS

| Path-loss Type | Usage Model | Note |
|---|---|---|
| Type-E | I,III,IV | Only one node is ART(NLOS) |
| Type-F | I,III,IV | Both node are BRT(LOS,NLOS) |

*Tab. 5.2:* Additional path loss model in IEEE 802.16j networks

is BRT. The COST 231 Walfisch-Ikegami model is recommended. The Cost 231 W-I model is fully matching the measured results for urban areas, and gives the suitable building size and rooftop heights. It can be used for both suburban and urban areas.

For Type-F, it is classified into two cases: LOS case and NLOS case. For LOS case, it assume that both MS's antenna and RS/BS's antenna are located below the rooftop, and that they are located on the same street. The path loss will be different if the antenna heights of RS/BS and MS is different. In addition, a visibility factor is included which influence path loss further than distance increases. Thus, to judge a link belongs to LOS or NLOS could not only depending on the distance but also considering visibility factor. For Type-F NLOS case, it assume both nodes antenna heights are below rooftop and they are located on different streets. The visibility factor still be included to compatible to the LOS case.

Since the link may be either LOS or NLOS in Type-F case, how to determine whether it's LOS or NLOS link is a key issue. The following equation for LOS probability is considered in our simulation:

$$P_{LOS}(d) = \begin{cases} 1 & , \quad d \leq 15m, \\ 1 - (1 - (1.56 - 0.48 \cdot log_{10}d)^3)^{\frac{1}{3}} & , \quad d > 15m \end{cases}$$

where $d = \sqrt{d_1^2 + d_2^2}$, and $d_1$ and $d_2$ are shown in Fig. 5.2.

## 5.3 Relative Movement Indicator of Mobile Station

The RMI is estimated by comparing the value of observed frame duration $(T'_{fd})$ and the system predefined frame duration $(T_{fd})$. For one OFDM-based wireless relay networks, system predefined frame duration is determined as well as data symbol number being chosen by RS or BS. In our considered case, the observed frame duration
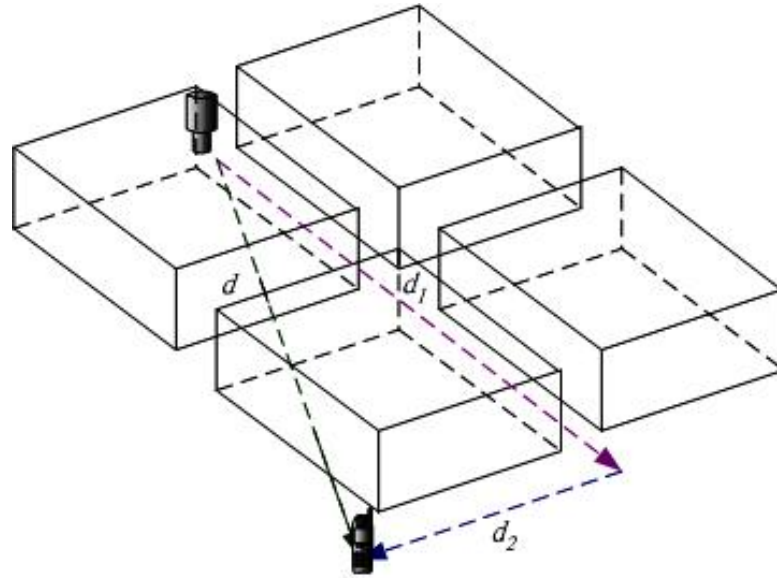
*Fig. 5.2:* Example of path-loss Type-F.

of MS may be change because of the MS's movement. The difference between observed frame duration and system predefined duration provides an extra information to describe the relative movement between MS and target RS/BS. This information can help for select the target station while handoff occurs.

The traditional approach of relative movement estimation is usually accomplished in the MAC layer, such as round-trip time. This approach is not fast and accurate enough. We provide a fast estimation scheme by using the pure PHY-layer technique which proposed in Chapter 3 and Chapter 4.

The complete process of RMI estimation is shown in Fig. 5.3. We get the frame arrival time quickly and accurately by using the technique which provided in Chapter 3 and Chapter 4. The observed frame duration is equal to the time interval between two frame arrival time (or called frame inter-arrival time). If MS is moving, the relative movement will change the frame inter-arrival time (i.e the observed frame
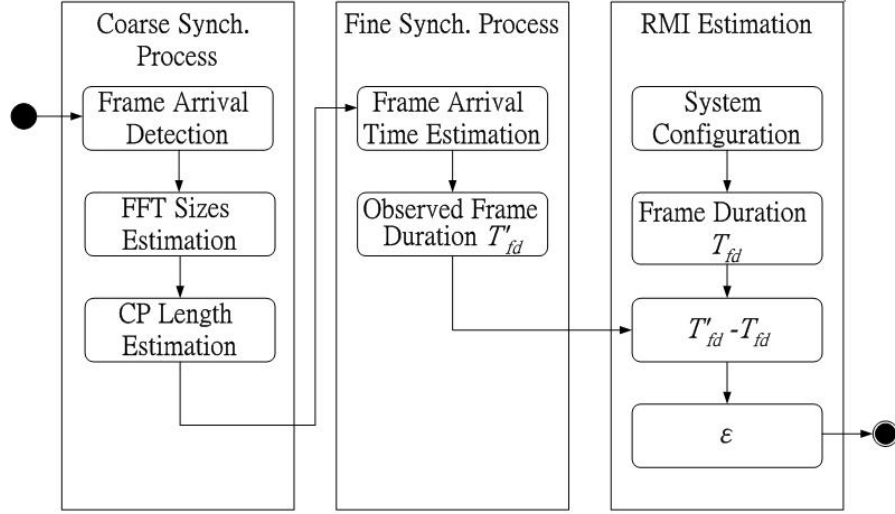
Fig. 5.3: The complete process to estimate the RMI.

duration). Finally, we can get the difference of observed frame duration and system predefined frame duration.

We also provide a frequency domain solution of RMI. From Chapter 3 and Chapter 4, we recall the system model:

$$r[k] \quad = \quad \frac{1}{\sqrt{N}} \sum_{n=0}^{N-1} x[n] e^{j\frac{2\pi nk}{N}} + n[k] \tag{5.1}$$

$$r^*[k] \quad = \quad e^{j\frac{2\pi kv}{N}} r[k] \tag{5.2}$$

where the subcarrier-frequency offset $v$ is a normalized value by the subcarrier spacing. In Chapter 3, we obtain the frame arrival event, FFT size $N_{FFT}$, CP ratio $\gamma$ and CP length $L$. In Chapter 4, we get the accurate frame arrival time as well as the timing offset $\hat{t}$. We can use these information to estimate the carrier-frequency offset. In the reference [35] and [36], a carrier-frequency offset estimator is provided. It is given by

$$\hat{v} = \frac{B}{2\pi} \sum_{m=1}^{B/2} w(m) \varphi(m) \tag{5.3}$$

where $B = \frac{1}{\gamma}$. The pre-factors

$$w(m) = 3\frac{4(B-m)(B-m+1) - B^2}{2(B^2 - 1)}, \ 1 \leq m \leq \frac{B}{2} \tag{5.4}$$

and the phase differences

$$\phi(m) = [arg\{R_r(m)\} - arg\{R_r(m-1)\}]_{2\pi}, \ 1 \leq m \leq \frac{B}{2} \tag{5.5}$$

The coefficients

$$R_r(m) = \frac{1}{N_{FFT} - mM} \sum_{k=\hat{t}+mM}^{\hat{t}+N_{FFT}-1} r^*(k - mM)r(k), \ 0 \leq m \leq \frac{B}{2} \tag{5.6}$$

where $\hat{t}$ is the timing offset which can be estimated by comparing the observed start point of symbol and pre-defined start point of symbol. Since

$$T'_{fd}(t) = T_{fd}(\frac{\nu}{c})\cos(\theta(t)) \ (time \, domain) \tag{5.7}$$

$$f'_{sc}(t) = f_{sc}(\frac{\nu}{c})\cos(\theta(t)) \ (frequency \, domain) \tag{5.8}$$

where $f_{sc}$ is the subcarrier spacing. If the angel $\theta(t)$ between movement direction and target station is equal, the only influential factor is the mobile's velocity $\nu$. Thus, the impact of mobility on the difference of frame inter-arrival time and the normalized subcarrier frequency offset is equivalent.

We called the difference of frame inter-arrival time and normalized subcarrier frequency offset as RMI ($\varepsilon$), and give a numerical definition as follows:

$$\hat{\varepsilon}_t = T'_{fd}(t) - T_{fd} \tag{5.9}$$

$$\hat{v}_t = f_{sc} - f'_{sc}(t) \tag{5.10}$$

The value of $\varepsilon$ could be positive, zero or negative. It physical meaning can be concluded as follows:

1. $\hat{\varepsilon}_t, \hat{v}_t < 0$ :

   the MS is moving toward to the target station.

2. $\hat{\varepsilon}_t, \hat{v}_t = 0$ :

   there is no relative movement between MS and candidate target station.

3. $\hat{\varepsilon}_t, \hat{v}_t > 0$ :

   the MS is moving away from the target station.

## 5.4 Proposed Difference of Frame Inter-arrival Time Based Target Selection Algorithm

We proposed a difference of frame inter-arrival time based target selection algorithm to solve the issue of handoffs frequency increasing. The basic concept is to introduce the mobility pattern into target selection decision. By doing so, the radio link between MS and target station could be hold for a longer time. The handoff frequency will be decreased as well.

In the reference [1], a technique was proposed to reduce inter-cell handoff but may increase intra-cell handoff events. Another issue in the reference [1] is that the controlling of inter-cell and intra-cell handoff rely on broadcasting the cell-ID or network topology information, which may induce a lot of signaling overhead.

In the IEEE 802.16j networks, hard handoff must be supported, and fast base station switch (FBSS) and macro diversity handoff (MDHO) are optional. Here, we discuss the hard handoff case. The criteria of conventional target selection algorithm in hard handoff is based on the RSSI, or carrier to interference plus noise ratio (CINR). We introduce RMI to MS's handoff criteria which could offer more information to help MS make a better choice of target station while handoff procedure occurs.

First, we give a general form of mixed indicators to represent the new evaluation criteria:

$$H_t \;=\; (1 + \boldsymbol{\alpha} \cdot \frac{\hat{\boldsymbol{\varepsilon}}_t}{\boldsymbol{\varepsilon}_{max}}) \cdot RSSI_t \tag{5.11}$$

$$=\; (1 + \boldsymbol{\alpha} \cdot \frac{\hat{\boldsymbol{v}}_t}{\boldsymbol{v}_{max}}) \cdot RSSI_t \tag{5.12}$$

where $H_t$ is the monitored quality criteria, $\alpha$ is the weight factor, $\hat{\varepsilon}_t$ and $\hat{v}_t$ is estimated RMI at time $t$, $\varepsilon_{max}$ and $v_{max}$ is the maximum value of RMI under specific velocity. In the references [2] [3], RSSI reported by MS shall be quantized in 1 dB increments, ranging from -40 dBm to -123 dBm, totally 84 steps. Values outside this range shall be assigned the closest extreme value within the scale. In order to joint the mobility information to the target selection decision, we could normalize RMI by dividing its maximum value, and give a weight $\alpha$ to adjust its impact capability to the original RSSI value.

## 5.5 Simulation Result

In this simulation, the whole simulation are running by the baseband signal. All system parameters are defined in the Table 5.3.

The main factors which influence the handoff number becomes: velocity of MS $\nu$, weight factor $\alpha$ and RS deployment model. The simulation result is shown in Fig. 5.4 and Fig. 5.5 and concluded as follows:

1. Uniform distribution:

   This kind of deployment model could get a uniform received signal strength, the received signal strength dropping slowly with increasing of $\alpha$, thus we can see the outage probability always closed to 0 under any $\alpha$ value. The reduced handoff

frequency ratio is more than 50 percent under any MS velocity. Thus, the proposed approach could reduce handoff frequency significantly.

2. Non-uniform distribution:

   This kind of deployment model may cause the worse received signal strength. The mean RSSI is lower than uniform distribution model, so does the outage probability. The Outage probability is growing with $\alpha$ value, the reason is that once $\alpha$ getting large, MS will determine to execute handoff very early, but the RSSI of original serving station may still stronger than handoff target station. In the other hand, outage probability can still keep in 0 if $\alpha$ is smaller than 10 and 15 under velocity 30 km/hr and 60 km/hr. In the mean time, the handoff frequency reduce ratio is about 0.75 to 0.5. This could proof that proposed approach could significantly improve the handoff performance.

## 5.6  Conclusion

In this chapter, we proposed a time-of-arrival based target selection algorithm to reduce handoff frequency while MS moving in the Manhattan-like urban environment. We first provide a system model to simulate a urban environment. In this model, we introduce new additional path loss models. Second, we mixed RSSI and RMI into a new handoff criterion to instead of pure RSSI measurement for target selection of handoff process.

According to the simulation results, the proposed algorithm performs well with respect to reduce handoff frequency significantly. For the further work, the adaptive algorithm to minimize handoff reduce ratio and outage probability should be studied.

| Parameters | Value |
|---|---|
| Antenna Type | Omni |
| Thermal Noise | $-174\,dBm$ |
| Power | $BS = 46\,dBm, RS = 40\,dBm$ |
| $N_{FFT}$ | 1024 points |
| Channel Bandwidth $BW$ | 5 MHz |
| Sampling Rate $F_s$ | $=5^*(8/7)$=5.7143   MHz |
| Sub-Carrier Spacing $f_{sc}$ | $=F_s/N_{FFT}$=5.5804 kHz |
| OFDMA Symbol Time $T_{sb}$ | $=1/\Delta_f = 179.2\,\mu s$ |
| Sampling Time $T_{sp}$ | $=T_{sb}/N_{FFT} = 0.175\,\mu s = 175\,ns$ |
| Guard Time $T_g$ | $=(1/4)^*T_{sb} = 44.8\,\mu s$ |
| Overall Symbol Time $T_s$ | $=(5/4)^*T_{sb} = 224\,\mu s$ |
| Frame Duration $T_{fd}$ | $=20^*T_s = 4.5\,ms$ |
| MS Velocity | 30 Km/hr, 60 Km/hr |
| Simulation Time | 250 second |

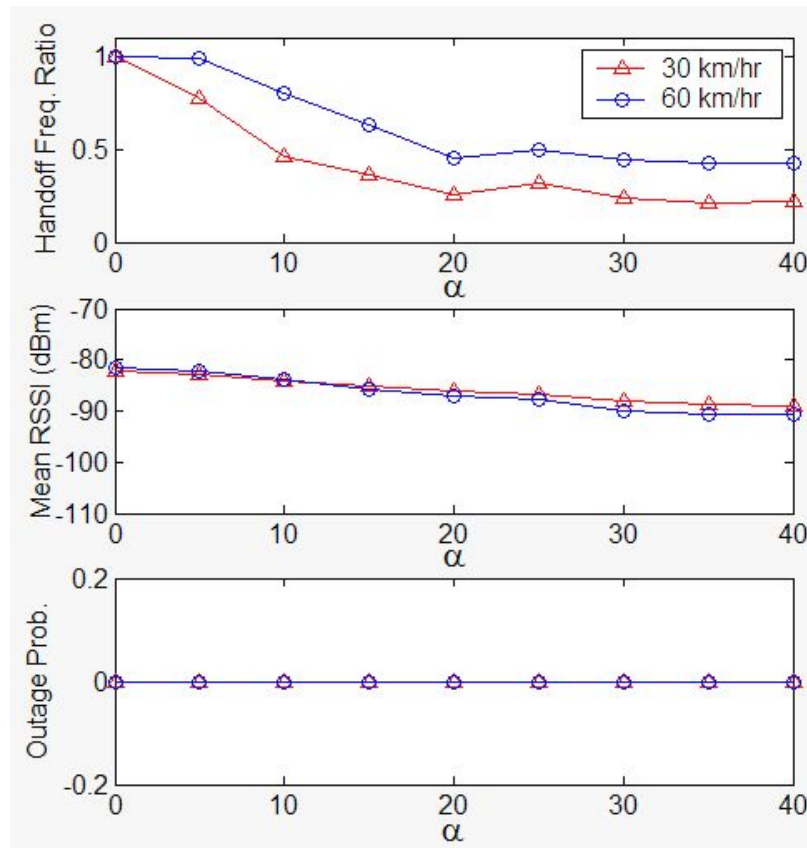Tab. 5.3: System parameters

Fig. 5.4: Simulation result under uniform distribution of RS
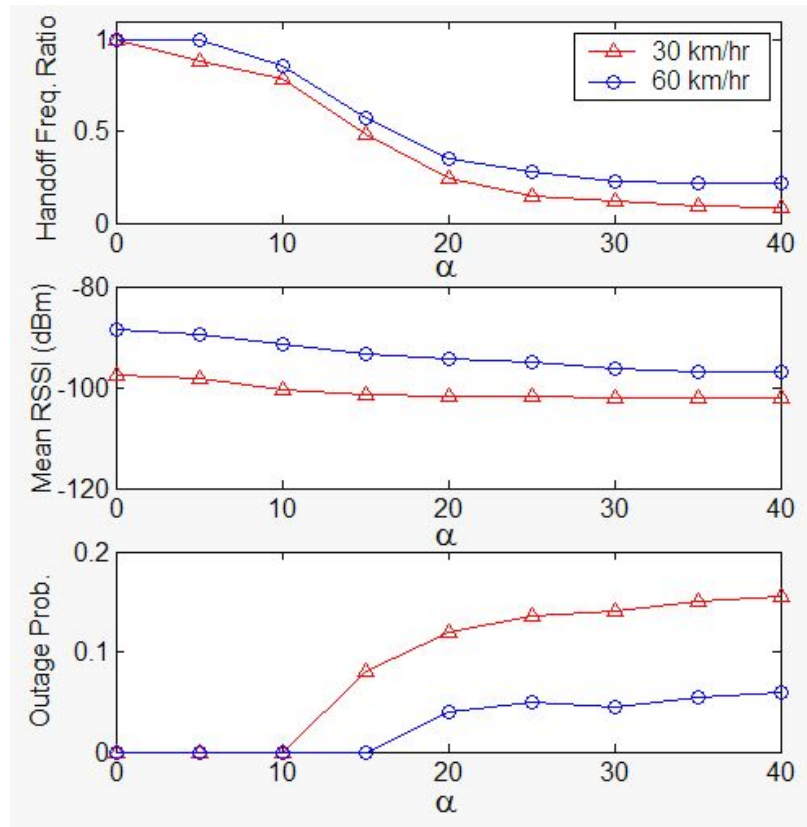
*Fig. 5.5:* Simulation result under non-uniform distribution of RS

# CHAPTER 6

# Concluding Remarks

The objective of this thesis is to efficiently select a target station to reduce handoff frequency while the RS is widely deployed in the urban environment, and MS is moving around it. we concluding our research result as follows.

## 6.1　OFDM Frame Arrival Time Estimation based on Fast PHY-layer Schemes for Obtaining CP Lengths and FFT Sizes

In Chapter 3, we described the synchronization technique and relative problem. We utilize the conjugated symmetric characteristics of BPSK modulated preamble, and provide a average difference of auto-correlation value based algorithm to accomplish frame arrival detection and the estimation of FFT size and CP length.

In Chapter 4, we investigate the frame arrival time estimation. It is accomplished by reversing first half part of received signal and then make correlation with the rest signal. We also provide a zero-forcing (ZF) pre-FFT equalizer to eliminate

delay spread under SUI-3 channel.

## 6.2 Difference of Frame Inter-arrival Time Based Target Selection Scheme for Reducing Handoffs in Wireless Multi-hop Relay Networks

In Chapter 5, we propose a RMI estimation scheme to represent the mobility pattern of MS. We first provide a system model to simulate a urban environment. In this model, we introduce some new additional path loss models used in IEEE 802.16j networks. Second, we mixed RSSI and RMI into a Time-of-Arrival based target selection scheme. At the last, we compare the handoff performance (handoff frequency) between conventional target selection scheme and proposed scheme to proof that the proposed scheme is better than conventional method.

## 6.3 Suggestion for Future Work

For the future research of the thesis, we provide the following suggestions to extend our work:

- Consider others optional handoff scheme like *Fast Base Station Switch* (FBSS) and *Macro Diversity Handoff* (MDHO).

- Study how the proposed approach influences the performance of upper layer protocol, such as ARQ efficiency, packet throughput, QoS, sleep mode power saving, etc. This could be helpful for real system design.

- Consider the tree-based structure of IEEE 802.16j multi-hop relay network, we care about the handoff latency on MAC layer.

# Bibliography

[1] J. H. Park, K.-Y. Han, and D.-H. Cho, "Reducing Inter-Cell Handover Events based on Cell ID Information in Multi-hop Relay Systems," *Vehicular Technology Conference, 2007. VTC2007-Spring. IEEE 65th*, pp. 743–747, 22-25 April 2007.

[2] IEEE Std. 802.16-2004, "IEEE Standard for Local and Metropolitan Area Networks -Part 16: Air Interface for Fixed Broadband Wireless Access Systems," October 2004.

[3] IEEE Std. 802.16e, "IEEE Standard for Local and Metropolitan Area Networks -Part 16: Air Interface for Fixed Broadband Wireless Access Systems -Amendment 2: Physical and Medium Access Control Layers for Combined Fixed and Mobile Operation in Licensed Bands and Corrigendum 1," February 2006.

[4] R. Pabst, B. Walke, D. Schultz, P. Herhold, H. Yanikomeroglu, S. Mukherjee, H. Viswanathan, M. Lott, W. Zirwas, M. Dohler, H. Aghvami, D. Falconer, and G. Fettweis, "Relay-based Deployment Concepts for Wireless and Mobile Broadband Radio," *Communications Magazine, IEEE*, vol. 42, Issue 9, pp. 80–89, Sept. 2004.

[5] IEEE 802.16's Relay Task Group, "http://ieee802.org/16/relay/."

[6] IEEE C802.16j-06/015, "Harmonized Contribution on 802.16j (Mobile Multihop Relay) Usage Models," Sept. 2006.

[7] IEEE C802.16j-06/217, "Overview of the Proposal for MS MAC Handover Procedure in an MR Network," Nov. 2006.

[8] IEEE C802.16j-06/166, "Network Topology Advertisement for IEEE 802.16j," Nov. 2006.

[9] IEEE C802.16j-06/220, "MS MAC Handover Procedure in an MR Network-Handover Execution," Nov. 2006.

[10] IEEE C802.16j-06/218, "MS MAC Handover Procedure in an MR Network-Network Topology Acquisition and MS Scanning," Nov. 2006.

[11] IEEE C802.16j-06/219, "MS MAC Handover Procedure in an MR Network-Handover Decision and Initiation," Nov. 2006.

[12] IEEE C802.16j-06/221, "MS MAC Handover Procedure in an MR Network-Termination," Nov. 2006.

[13] IEEE C802.16j-07/072, "MS Handover with Non-transparent RS," May. 2007.

[14] C. Hoymann, K. Klagges, and M. Schinnenburg, "Multihop Communication in Relay Enhanced IEEE 802.16 Networks," *IEEE International Symposium on Personal, Indoor and Mobile Radio Communications*, pp. 1–4, Sep. 2006.

[15] IEEE C802.16j-07/177, "In-band Non-transparent Relay Frame Structure," Mar. 2007.

[16] Y. Okumura, E. Ohmori, T. Kawano, , and K. Fukua, "Field Strength and Its Variability in UHF and VHF Land-mobile Radio Service," *Rev. Elec. Commun. Lab.*, vol. 16, no.9, 1968.

[17] M. Hata, "Empirical Formula for Propagation Loss in Land Mobile Radio Services," *IEEE Trans. Veh. Technol.*, vol. 29, pp. 317–325, Aug. 1980.

[18] EURO-COST-231 Revision 2, "Urban Transmission Loss Models for Mobile Radio in the 900 and 1800 MHz Bands," *Rev. Elec. Commun. Lab.*, Sept. 1991.

[19] V. E. et. al, "An Empirically Based Path Loss Model for Wireless Channels in Suburban Environments," *IEEE JSAC.*, vol. 17, no.7, pp. 1205–1211, July. 1999.

[20] M. Smith and J. Dalley, "A New Methodology for Deriving Path Loss Models from Cellular Drive Test Data," *Proc. AP2000 Conference, Davos, Switzerland.*, Apr. 2000.

[21] IEEE 802.16.3c-00/49r2, "Interim Channel Models for G2 MMDS Fixed Wireless Applications."

[22] IEEE 802.16.3c-01/29, "Channel Models for Fixed Wireless Applications."

[23] A. Peled and A. Ruiz, "Frequency Domain Data Transmission Using Reduced Computational Complexity Algorithms," *IEEE ICASSP Conf.*, vol. 5, pp. 964–967, Apr. 1980.

[24] H. Bolcskei, M. Borgmann, and A. J. Paulraj, "Impact of the Propagation Environment on the Performance of Space-Frequency Coded MIMO-OFDM," *IEEE J. Select. Areas Commun.*, vol. 21, no. 3, pp. 427– 439, Apr. 2003.

[25] T. Schmidl and D. Cox, "Robust Frequency and Timing Synchronization for OFDM," *IEEE Transactions on Communications*, vol. 45, pp. 1613–1621, Dec. 1997.

[26] H. Minn and V. Bhargava, "A simple and Efficient Timing Offset Estimation for OFDM Systems," *Vehicular Technology Conference Proceedings, 2000. VTC 2000-Spring Tokyo. 2000 IEEE 51st*, vol. Volume 1, pp. 51–55, May. 2000.

[27] B. Park, H. Cheon, and C. K. D. Hong, "A Simple Preamble for OFDM Timing Offset Estimation," *Vehicular Technology Conference, 2002. Proceedings. VTC 2002-Fall. 2002 IEEE 56th*, vol. Volume 2, 24-28, pp. 729–732, Sep. 2002.

[28] S. D. Choi, J. M. Choi, and J. H. Lee, "An Initial Timing Offset Estimation Method for OFDM Systems in Rayleigh Fading Channel," *Vehicular Technology Conference, 2006. VTC-2006 Fall. 2006 IEEE 64th*, pp. 1–5, Sept. 2006.

[29] W. Akmouche, S. Gruffaz, and A. Quinquis, "Blind Equalization of OFDM Signals on HF-channels," *Signals, Systems and Computers, 2000. Conference Record of the Thirty-Fourth Asilomar Conference on Volume 2*, pp. 1806 – 1810, 29 Oct.- 1 Nov 2000.

[30] S. Yatawatta and A. Petropulu, "Blind Channel Equalization in a Multiuser OFDM Communications System," *Signals, Systems and Computers, 2002. Conference Record of the Thirty-Sixth Asilomar Conference on Volume 2*, pp. 1709 – 1713, 3-6 Nov 2002.

[31] T. Kim and I. Eo, "Blind Channel Estimation and Equalization in OFDM System With Circular Precoding," *Acoustics, Speech and Signal Processing, 2006. ICASSP 2006 Proceedings. 2006 IEEE International Conference on Volume 4*, pp. IV–IV, 14-19 May 2006.

[32] "Selection Procedure for the Choice of Radio Transmission Technologies of the Universal Mobile Telecommunications System (UMTS 30.03)," *Tech. Rep. ETSI TR 101 112 v.3.2.0, ETSI SMG2*, Apr. 1998.

[33] IEEE C80216mmr-06/003, "On the Throughput Enhancement of Fixed Relay Concept in Manhattan-like Urban Environments," Jan. 2006.

[34] IEEE C802.16j-06/013, "Multi-hop Relay System Evaluation Methodology(Channel Model and Performance Metric)," Feb. 2007.

[35] H. Minn, V. Bhargava, and K. Letaief, "A Robust Timing and Frequency Synchronization for OFDM Systems," *Wireless Communications, IEEE Transactions on Volume 2, Issue 4*, pp. 822–839, July 2003.

[36] M. Morelli and U. Mengali, "An Improved Frequency Offset Estimator for OFDM Applications," *Communications Letters, IEEE Volume 3, Issue 3*, pp. 75–77, March 1999.

# Vita

**Cheng-Min Chen** was born in Taiwan in 1972. He received the B.S. degree in the Department of Nuclear Engineering and Engineering Physics from National Tsing Hua University, HsinChu, Taiwan in 1996. He obtained his M.S. degree in the Wireless Network Lab. of the Department of Communication Engineering at National Chiao Tung University in Auguest of 2008. From July 2000 to present, he has been a researcher in Telecommunication Laboratories (TL) of Chunghwa Telecom Co., Ltd. (CHT). His research interests are in the fields of wireless communication systems, mobile application, VoIP, IMS, queuing network, etc. You can contact with him via e-mail: jimmypoet@gmail.com.